Pathological Study on the Possible Pathogenesis of Seizure-Induced Neuronal Death in the Epileptic Brain

てんかん発作により脳に生じる

神経細胞死の病理発生に関する病理学的研究

Masashi Sakurai

Thesis submitted to the United Graduate School of Veterinary Science at Yamaguchi University in partial fulfillment of the requirements for the degree of Doctor of Philosophy

Takehito Morita, Ph.D., Chair
Kenji Takahashi, Ph.D.
Masahiro Morimoto, Ph.D.
Takashi Takeuchi, Ph.D.
Tomohiro Imagawa, Ph.D.

The United Graduate School of Veterinary Science
Yamaguchi University

2015

ABSTRACT

Pathological Study on the Possible Pathogenesis of Seizure-Induced Neuronal Damage in the Epileptic Brain

Masashi Sakurai

Epilepsy is a chronic neurological condition characterized by recurrent seizures. Anti-epileptic drugs are major therapies for treatment of epileptic patients. However, these drug therapies target its symptoms rather than the underlying cause. Approximately 30 percent of epilepsy patients do not have seizure remission despite appropriate drug therapies (intractable epilepsy). In addition to the recurrent seizures, the intractable epilepsy patients have been reported to suffer from sequellae of brain dysfunctions, such as memory loss, language impairment, depression and olfactory dysfunction. These brain dysfunctions are considered to be caused by seizure-induced neuronal death. However, the pathogenesis of seizure-induced neuronal death was still unknown. To investigate a possible pathogenesis of seizure-induced neuronal death, the cerebrum of the familial Shetland Sheepdogs and kainic acid-treat rat (an animal model

of epilepsy) was examined using histopathological and immunohistochemical methods. In the cerebrum of the familial Shetland Sheepdogs, angiogenesis and microglial activation were found consistent with the distribution of seizure-induced neuronal death with glutamate transporter 1 (GLT-1) downregulation. In the cerebrum of kainic acid-treated rat, GLT-1 downregulation and microglial activation was found consistent with the distribution of seizure-induced neuronal death. Further, these pathological changes were observed in the same regions before neuronal death was detected. These results indicate that seizures can induce various pathological changes in the brain after seizures, which includes both neuroprotective (angiogenesis) and neurodestructive effects (microglial activation and GLT-1 downregulation). Glutamate excitotoxicity due to GLT-1 downregulation is considered to be a cause of seizure-induced neuronal death. The information from these studies may lead to deeper understanding of epilepsy and development of treatment for epilepsy.

TABLE OF CONTENTS

GENERAL INTRODUCTION AND BACKGROUND

1. Epilepsy

Epilepsy is a chronic neurological condition characterized by recurrent seizures due to neuronal hyperactivity (Blume et al., 2001). With its high prevalence, epilepsy is highly interested neuronal disease in the world (4 to 10 per 1,000 persons) (Sander et al., 2003). Anti-epileptic drugs are major therapies for treatment of epileptic patients. However, these drug therapies target its symptoms rather than the underlying cause. Moreover, approximately 30% of epilepsy patients do not have seizure remission despite appropriate drug therapies (intractable epilepsy) (Kwan et al., 2000).

Temporal lobe epilepsy (TLE), refers to an electroclinical syndrome in which seizures arises from the temporal lobe. TLE is a prominent and prevalent epilepsy syndrome in children, adolescents and adults (Goldberg et al., 2013).

2. Seizure-induced neuronal death and brain dysfunctions

Recurrent seizure without interictal resumption or “status epilepticus” is known to induce neuronal death in the cerebrum (Fujikawa et al., 2000; Meldrum et al., 1993). In the cerebrum of TLE patients and animal models of TLE, seizure-induced neuronal

death spread in the limbic and limbic-related structures where seizure activity arises from (Duncan, 2002; Holmes, 2002). In addition to the recurrent seizures, TLE patients has been reported to suffer from sequellae of brain dysfunctions, such as memory loss, language impairment, depression and olfactory dysfunction (Alessio et al., 2006; Jacek et al., 2007; Kanner et al., 2011). Limbic and limbic-related structures have an important role in memory, language, decision-making and olfactory functions (McKenna et al., 2004; Tham et al., 2009; Vertes et al., 2002). The seizure-induced neuronal death in limbic and limbic-related structures may be responsible for the sequellae (Figure 1). However, the pathogenesis underlying seizure-induced neuronal death remains still unclear.

3. Possible Pathogenesis of seizure-induced neuronal death

Recent studies suggest that there are several pathological changes underlying seizure-induced neuronal death in epileptic brains (Figure 2).

3.1. Glutamate excitotoxicity

Glutamate is known as an excitatory neurotransmitter that relates number of essential phenomena associated with neural functions. On the other hand, glutamate is

also known as a neurotoxin that induces neuronal degeneration and neuronal death due to overstimulation of glutamate receptors (Balkhi et al., 2014).

In epileptic brain, electroencephalography (EEG) analysis shows epileptic discharges that indicate neuronal hyperexcitation during seizures and also interictal period (Herman et al., 2011; Salami et al., 2014). Seizure-induced neuronal death is distributed along with the regions where seizure activity arises from (Duncan, 2002; Holmes, 2002). Further, glutamate transporter 1 (GLT-1) has been reported to be downregulated in epileptic brains (Proper EA et al., 2002; Dutuit M et al., 2002; Samuelsson C et al., 2000). GLT-1 is important for astrocytic glutamate uptake and GLT-1 downregulation has been reported to induce glutamate excitotoxicity (Rothstein et al., 1994; Sonnewald et al., 1997). Therefore, glutamate excitotoxicity might play an important role in the induction of seizure-induced neuronal death in epileptic brain.

3.2. Seizure-induced blood flow alterations

Recent papers describe dynamic blood flow alternation in the epileptic brain during seizures (Dupont et al., 2009), and focal hypoperfusion has been considered as a cause of neuronal death (Choy et al., 2010). Hypoperfusion and ischemia are well known to induce neuronal death in the brain (Walton et al., 1999). It is possible that a local

hypoperfusion or ischemia is part of the pathophysiological process that underlies the seizure-induced neuronal death.

3.3. Blood-brain barrier breakdown

Blood–brain barrier is a structure that limits the penetration of a variety of substances from the blood into the brain. This structure is composed of vascular endothelium and astrocytic feet, and protects brain physically and physiologically (Abbott et al., 2010). Recent papers describe that an increase of blood-brain barrier permeability that leads to blood-brain barrier breakdown occurs in the cerebrum of animal models of epilepsy (Oby et al., 2006). Further, blood-brain barrier breakdown has been reported to relate with the progression of epilepsy (van Vliet et al., 2007).

3.4. Neuroinflammation (glial activation)

In the epileptic brain, glial cell (mostly microglia and astrocytes) has been reported to be activated focally by seizures (Wetherington et al., 2008; Rizzi et al., 2003). These activated glial cells express pro-inflammatory cytokines, such as tumor necrosis factor alpha, interleukin 1 beta and interleukin 6 (Vezzani et al., 2008a). The pro-inflammatory cytokines has been reported to induce neurodegenerative effects (Brown et al., 2010; Vezzani et al., 2008b; Rijkers et al., 2009). Also, nitric oxide synthase expression in the

activated glial cells suggests oxidative stress to neuros in the epileptic brain (Herberg et al., 1995).

4. Epilepsy in animals

Epilepsy is one of the most common neuronal diseases also in animals (Thomas, 2010). As same as human epilepsy, anti-epileptic drugs are major therapies for epileptic animals and there are some reports of intractable epilepsy in animals (Buckmaster, et al., 2002). Histologically, neuronal death is a characteristic finding in the cerebrum of epileptic animals (Morita et al., 2002; Kuwabara et al., 2010).To our knowledge, no brain dysfunctions are reported in epileptic animals, however, some report demonstrates learning deficits and depression-like behaviors in an animal model of epilepsy (Lee et al., 2001; Sarkisova,2003).

4.1. Familial epileptic Shetland Sheepdogs in Tottori University (Figure 3)

In the department of Veterinary Pathology in Tottori University, familial epileptic Shetland Sheepdogs are kept. These familial dogs clinically showed epileptic discharges on EEG analysis, however, some of them had seizures while others did not. Histological examination revealed that neuronal death was present in the specific regions of the cerebrum of the dogs having seizures (Morita et al., 2002). In addition to the seizure-

induced neuronal death, immunohistochemistry suggested that GLT-1 downregulation had strong relationship to the neuronal death (Morita et al., 2005). As described above , GLT-1 downregulation has been reported to induce glutamate excitotoxicity (Rothstein et al., 1994; Sonnewald et al., 1997). Threrefore, GLT-1 downregulation is considered to be a cause of the seizure-induced neuronal death in the cerebrum of familial epileptic Shetland Sheepdogs.

5. Animal models of epilepsy

In rodents (rats and mice), status epilepticus can be initiated by use of electrical stimulation (kindling) or chemical convulsants (Buckmaster, 2004). In the cerebrum of these animal models, several pathological changes including neuronal death and glial activation have been reported to be similar to those of humans (Buckmaster, 2004; Curia, et al., 2008; Levesque et al., 2013)

6.1. Kindling model (Figure 4)

Kindling means repeated, mild, electrical stimulation of the limbic or limbic-related structures, such as amygdala, olfactory regions and hippocampus, to induce a progressive and permanent seizure response. With repeated stimulation, after discharges extented and rats began displaying recurrent seizure (status epilepticus), despite

unaltered stimulation parameters (Morimoto et al., 2004). Then, after a latent period, many of the animals start to show spontaneous recurrent seizures (Buckmaster, 2004).

6.2. Chemical induction models (Figure. 5)

Chemical convulsants such as pilocarpine and kainic acid can induce seizures in rodents. Pilocarpine is a muscarinic acethylcholine receptor agonist and kainic acid is a glutamate receptor agonist. Systemic injection of these chemicals can stimulate neurons in the brain and increases neuronal excitability, which results in recurrent seizures (status epilepticus) (Curia, et al., 2008; Levesque et al., 2013). Then, after an average latent period off approximately 26 days, many of the animals start to show spontaneous recurrent seizures (Buckmaster, 2004).

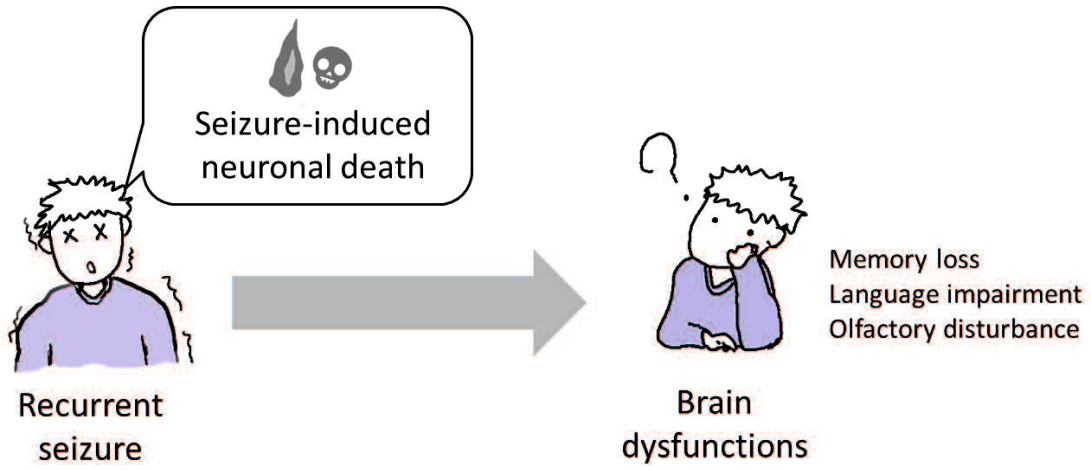

Figure 1. Schematic diagram shows the relationship between seizure-induced neuronal death and brain dysfunctions.

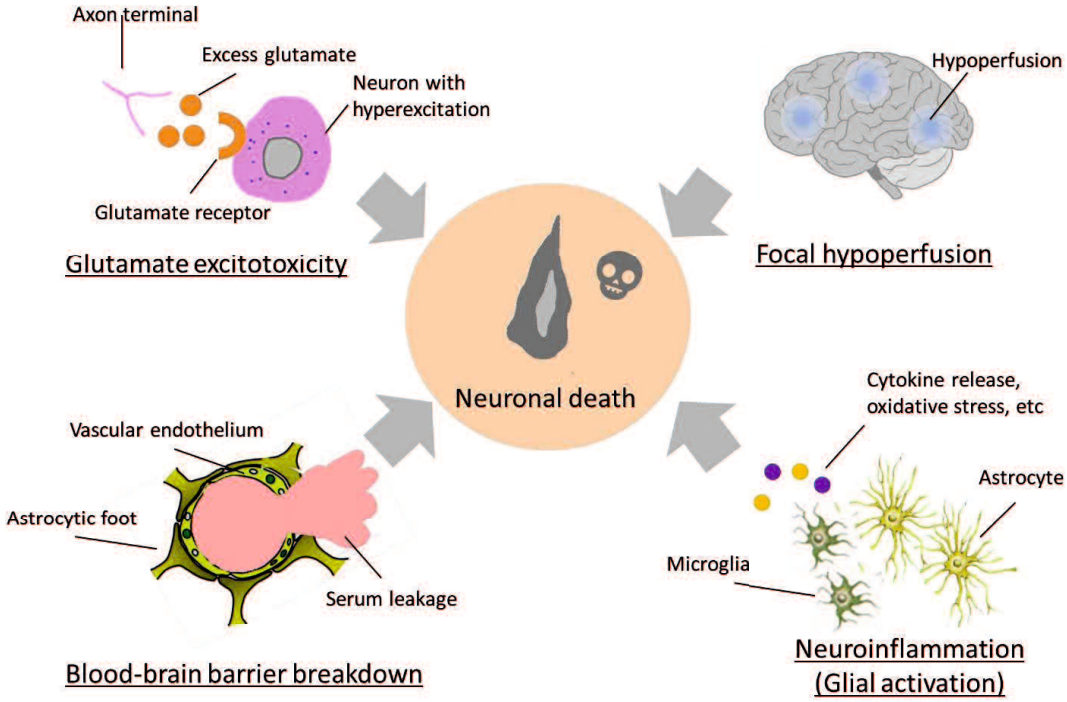

Figure 2. Schematic diagram of possible cause of seizure-induced neuronal death.

Several pathological changes are thought to underlie the mechanism of seizure-induced neuronal death in the epileptic brain during or after seizure.

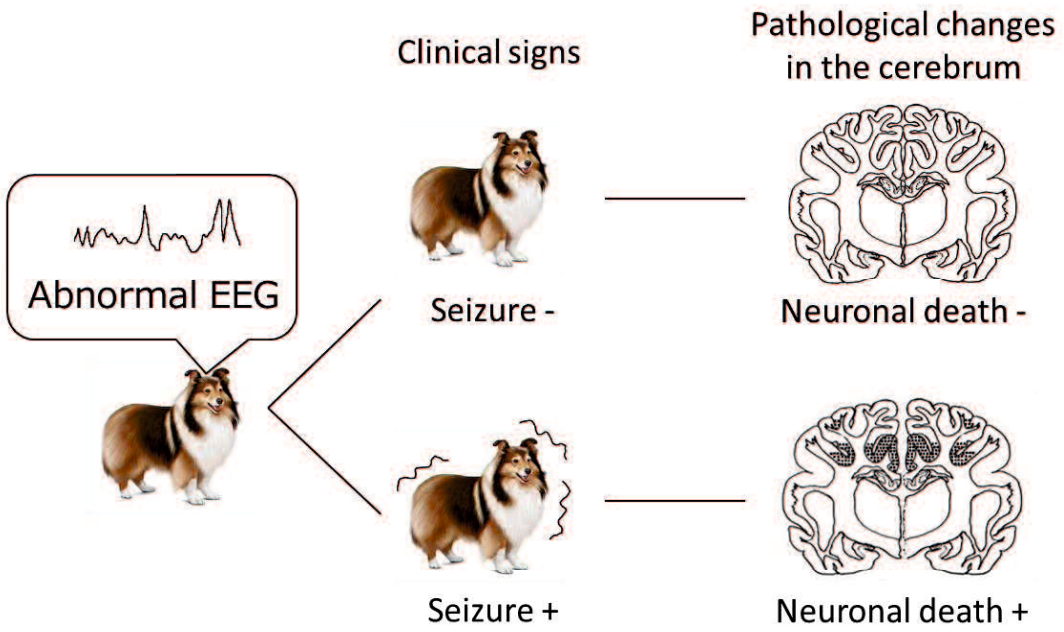

Figure 3. Clinical and histological findings of the familial Shetland Sheepdogs in Tottori University. All the dogs had abnormal electroencephalography, however, neuronal death was found only in the cerebrum of the dogs having seizures (black dot in coronal plane of the cerebrum).

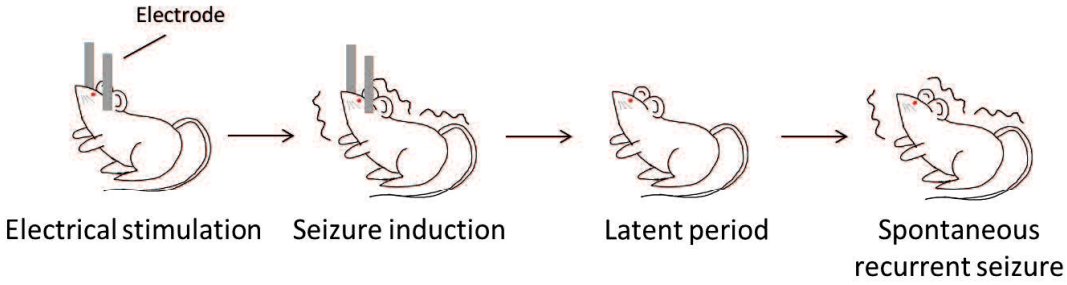

Figure 4. Schematic diagram of kindling model.

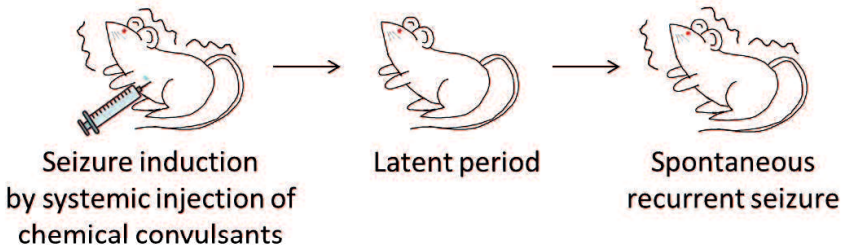

Figure 5. Schematic diagram of chemical induction model.

OBJECTIVE AND STRUCTURE OF THE THESIS

To study the possible pathogenesis of seizure-induced neuronal death, the cerebrums of Shetland Sheepdogs with familial epilepsy and kainic acid-treated rat were examined. GLT-1 expression was the most interested factor because the previous study in the cerebrum of the familial epileptic Shetland Sheepdogs strongly suggested the relationship between neuronal death and GLT-1 downregulation.

In chapter 1: To investigate pathological changes, which might be relevant to GLT-1 downregulation in the cerebrum of familial Shetland Sheepdogs, we performed histopathological and immunohistological examinations for angiogenesis and microglial activation.

In chapter 2: To investigate the lesions of neuronal death and GLT-1 downregulation at different time-points after seizures, we studied lesions in the thalamus of kainic acid-treated rat.

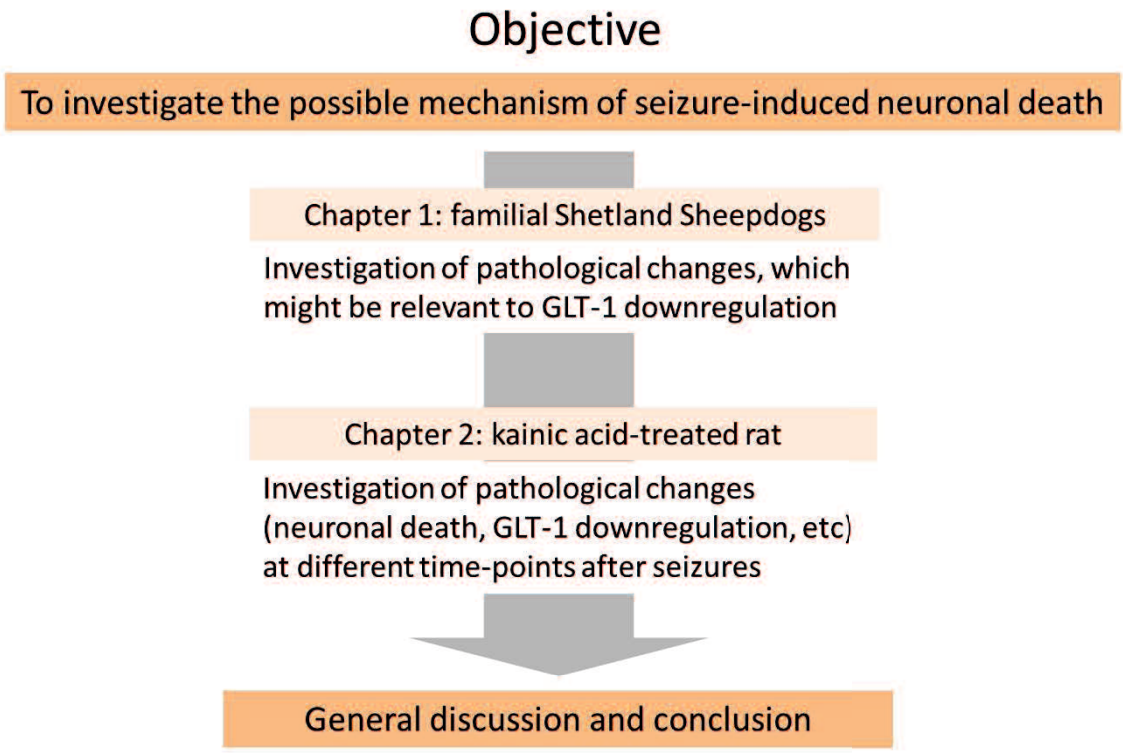

Figure. Structure of the thesis

LIST OF ORIGINAL PUBLICATIONS

The thesis is based on the following original publications.

Sakurai M., Morita T., Takeuchi T., and Shimada A. (2013). Relationship of angiogenesis and microglial activation to seizure-induced neuronal death in the cerebral cortex of Shetland Sheepdogs with familial epilepsy. *Am J Vet Res* **74**, 763-770.

Sakurai M., Kurokawa H., Shimada A., Nakamura K., Miyata H., and Morita T. (2014). Excitatory amino acid transporter 2 downregulation correlates with thalamic neuronal death following kainic acid-induced status epilepticus in rat. *Neuropathology* In press.

CHAPTER 1

Relationship of angiogenesis and microglial activation to seizure-induced neuronal death in the cerebrum of familial epileptic Shetland Sheepdogs

ABSTRACT

To examine angiogenesis and microglial activation in the cerebral lesion of familial epileptic Shetland Sheepdogs, ten dogs (six dogs with seizures and four dogs without seizures) were examined. Histological examination revealed that seizure-induced neuronal death was present in the cingulate cortex and cerebral cortex surrounding sulci. In and around the lesions, an increased number of microvessels was observed in the cerebrum of familial dogs with seizures. The microvessels appeared longer and more tortuous than those of dogs without seizures. Immunohistochemically, both neurons and glial cells in the lesions were positive for vascular endothelial growth factor (VEGF). Iba-1-positive microglia were also increased and morphologically activated in and around the lesions of seizure-induced neuronal death. Double immunofluorescence revealed that the activated microglia were positive for tumor necrosis factor-alpha, interleukin-6, and VEGF receptor 1. These findings were not observed in the cerebrum of familial dogs without seizures. Our results indicated that angiogenesis and microglial activation are thought to be related to seizure-induced neuronal death in the cerebrum of familial epileptic Shetland Sheepdogs. VEGF-induced microglial activation with pro-inflammatory cytokine production may accelerate seizure-induced neuronal death.

INTRODUCTION

Epilepsy is one of the most common neurological disorders in human and animals. Epileptic patients show chronic recurrent seizures and are sometimes associated with brain dysfunction (e. g. memory loss, language impairment and olfactory dysfunction) (Alession *et al*., 2006; Ciumas *et al*., 2008; Jacek *et al*., 2007). It has been reported that seizures induce neuronal death in the cerebrum human epilepsy and animal models of epilepsy (Fujikawa *et al*., 2000; Gorter *et al*., 2003; Wang *et al*., 2008). Seizure-induced neuronal death has been thought to be responsible for the brain dysfunction (Sutula et al., 1994). In addition, seizure-induced neuronal death has been reported to contribute the induction of subsequent seizures (Nairismägi *et al*., 2004; van Viet *et al*., 2004). However, the pathogenesis of seizure-induced neuronal death is still unknown, and an appropriate treatment for avoiding the seizure-induced neuronal death is not established.

Recently, seizure has been reported to induce angiogenesis and microglial activation, which are thought to be related to neuronal death (Rigau *et al*., 2008; Avignone *et al*., 2008; Crespel et al., 2002). Angiogensis is associated with an increase of local blood flow and is thought to be neuroprotective (Ndode-Ekane *et al*., 2010). However, VEGF, an important angiogenic factor, has neurodegenerative effects such as

induction of neuroinflammation and blood-brain barrier breakdown (Rigau *et al*., 2007; Croll *et al*., 2004). Neuroinflammation is the term used to describe the central nervous system inflammatory responses produced by activated glial cells. Activated microglia is major source of pro-inflammatory cytokines such as TNF-α and IL-6 (Vezzani *et al*., 2008). These cytokines are associated with neuronal damage in several neurological disorders, including epilepsy, Alzheimer's disease and amyotrophic lateral sclerosis (Allan *et al*., 2001; Heneka *et al*., 2010; Kiaei *et al*., 2006).

In a colony of familial epileptic Shetland Sheepdogs, all of the familial dogs showed abnormal activity on electroencephalography, but some dogs had seizures while others did not. The purpose of the current study is to examine whether angiogenesis and microglial activation are related to the seizure-induced neuronal death in the brain of familial epileptic Shetland Sheepdogs.

MATERIALS AND METHODS

Animals

Ten familial Shetland Sheepdogs and four age-matched non-familial Shetland Sheepdogs were used in this study. The familial dogs were classified into 2 groups; six familial dogs with a history of recurrent seizures ranging in age from 1 year 8 months to 5years (No. 1-6) and four familial dogs without seizure ranging in age from 1 year 9 months to 4 years 5 months (No. 7-10). In addition four non-familial Shetland Sheepdogs, ranging in age from 2 years 4 months to 4 years 7 months, were used as control dogs (No. 11-14). A previous study described about clinical history of the familial dogs with seizures (e.g. seizure onset, ictal period and seizure frequency) (Morita T *et al*., 2002). It was also described that all familial dogs (No. 1-10) showed abnormal activity on electroencephalography whereas 6 dogs (No. 1-6) with seizures histologically had acute neuronal change (ischemic-like change; shrunken eosinophilic cytoplasm and loss of nucleus) and astrocytosis in the cerebrum (Morita T *et al*., 2002). Clinically and histologically, no significant changes were detected in the brain of control dogs. A conventional vaccination schedule was followed and a monthly heartworm (*Dirofilaria immitis*) preventive treatment was administered. Appropriate

veterinary care was provided if a generalized seizure occurred. This study was carried out with the approval of the Animal Research Committee, in accordance with the guidelines for animal experimentation of the Faculty of Agriculture, Tottori University.

Histopathology and immunohistochemistry

Complete postmortem examination was performed on all the dogs, and systemic organs were fixed in 10% neutral phosphate-buffered formalin. Cerebral tissues were sectioned coronally in 4 mm intervals from the frontal lobe to the occipital lobe. The tissues were then routinely embedded in paraffin and sectioned at 4 μm for hematoxylin and eosin staining and immunohistochemistry.

Immunohistochemical analysis was performed with the labeled streptavidin-biotin (LSAB) method and the double-label immunofluorescence method, using primary antibodies listed in Table 1. After deparaffinization, the sections were transferred into citric acid buffer and boiled for 20 min at 98°C in a microwave (MI-77, Azuma, Tokyo, Japan) for antigen retrieval according to a standard microwave treatment protocol. For the LSAB method, after blocking endogenous peroxidase activity with 3% hydrogen peroxide for 15 min, sections were preincubated with 10% normal goat serum for 5 min in the microwave. Then, the sections were incubated with a primary antibody in

appropriate treatment for each antibody. Sections were sequentially incubated with biotinylated goat anti-rabbit IgG antibody (Dako, Glostrup, Denmark; diluted 1:400) or biotinylated goat anti-mouse IgG antibody (Dako; diluted 1:400) as a second antibody for 5 min in the microwave, and then incubated with peroxidase-labeled streptavidin complex (Dako) for 5 min in the microwave. The reaction was revealed using 3,3´-diaminobenzidine tetrahydrochloride (Dako). Sections were counterstained lightly with Mayer's hematoxylin. For the double-label immunofluorescence method, Alexa Fluor 488-conjugated goat anti-rabbit IgG antibody (Life technologies, Carlsbad, CA, USA; diluted 1:100) and Alexa Fluor 555-conjugated donkey anti-mouse IgG antibody (Life technologies; diluted 1:100) were used as second antibodies. After preincubation with normal goat serum for 5 min in the microwave, sections were incubated with rabbit anti-Iba-1 or rabbit anti- GFAP primary antibody, and then incubated with Alexa Fluor 488-conjugated goat anti-rabbit IgG second antibody for 1h at room temperature. Next, sections were incubated with an anti-mouse primary antibody (Table 1) and then incubated with Alexa Fluor 555-conjugated donkey anti-mouse IgG second antibody for 1h at room temperature. Sections were mounted in plain 80% tris-buffered glycerol. Analysis was performed with a confocal imaging system (AX-70, Olympus

Corporation, Tokyo, Japan). Nonspecific stain was estimated by replacing the primary antibody with phosphate-buffered saline.

Statistical analysis

Statistical analyses on severity of acute neuronal change, on number of microvessels and on relationship between the severity of acute neuronal change and the number of IL-6-positive cells were performed in the cingulate cortex of the familial dogs and control dogs. For the statistical analysis on severity of acute neuronal change, using a section stained with H&E stain (at the coronal level of corpus mamillare), each 5 fields of the cingulate cortex and cortex around the sulci (there were no overlaps) were randomly displayed at 200× magnification for each dog with seizure. Normal neurons (had large nucleus with prominent nuclear body and large cytoplasm with Nissl bodies) and neurons with acute change were counted, and the mean percentage of neurons with acute change was calculated. For the statistical analysis on number of microvessels, using a section immunohistochemically stained with vWF antibody (at the coronal level

of corpus mamillare), 10 fields of the cingulate cortex (there were no overlaps) were randomly displayed at 400× magnification for each case (BX-51, Olympus Corporation, Tokyo, Japan). The number of microvessels was counted. The mean number of microvessels was calculated for each case and each group and compared using the Student's t-test (normal distribution was checked by Kolmogorov-Smirnov test and equal variance was checked by F-test). For the statistical analysis on relationship between the severity of acute neuronal change and the number of IL-6-positive cells, the severity of acute neuronal change was defined by the number of neurons with acute change (in 400× magnification). The symbol "+" is used to indicate 5–¬¬9 neurons with acute change, "++" indicates 10–19 neurons with acute change, and "+++" indicates greater than 19 neurons with acute change. In the cerebrum of the familial dogs with seizures, 10 fields of each severity of acute neuronal change were randomly observed in 400× magnification and IL-6-positive cells were counted. The means number of IL-6-positive cells was calculated for each severity of acute neuronal change and compared

using the Student's t-test (normal distribution was checked by Kolmogorov-Smirnov test and equal variance was checked by F-test).

RESULTS

Histologically, acute neuronal change (ischemic-like change; shrunken eosinophilic cytoplasm and loss of nucleus) were observed in the cerebrum of the familial dogs with seizures, but not found in the cerebrum of either the familial dogs without seizures or control dogs (Fig. 1). The neurons with acute change were localized in the cingulate cortex and cerebral cortex surrounding sulci. In the familial dogs with seizures, microvessels appeared longer more and tortuous than those of the familial dogs without seizures in and around the areas of acute neuronal change (Fig. 2A, B). Occasionally, the microvessels were surrounded by oval to flat cells, which were immunohistochemically positive for vWF (Fig. 2C, D). In the cingulate cortex of the familial dogs with seizures, the number of microvessels was significantly increased compared to the familial dogs without seizures and control dogs, whereas there were no significant differences between the familial dogs without seizures and control dogs (Fig. 3). Immunohistochemically, in the familial dogs with seizures, glial cells and neurons were positive for VEGF in the cingulate cortex and cerebral cortex around sulci whereas VEGF-positive cells were not found in either the cerebrum of the familial dogs without seizures or control dogs (Fig. 4). The double-label immunofluorescence method

revealed that VEGF-positive glial cells were both Iba-1-positive microglia and GFAP-positive astrocytes (Fig. 5).

Comparing the familial dogs with seizures and the familial dogs without seizures, an increased number of Iba-1-positive microglia was detected in the cingulate cortex and cerebral cortex surrounding sulci in the familial dogs with seizures. These microglia were morphologically activated (i.e. had swollen cell bodies and longer processes) (Fig. 6). The double-label immunofluorescence method revealed that activated microglia were positive for VEGFR-1, TNF–α and IL-6 (Figs. 7A, 8A, 9A).

The distribution of VEGF-positive cells and activated microglia was similar to that of neurons with acute change, in addition, VEGF-positive cells and activated microglia were also observed in the areas surrounding neurons with acute change (Fig. 10).

In the familial dogs with seizures, IL-6-positive immunolabelings were detected not only in microglia but also in neurons (except neurons with acute change) and GFAP-positive astrocytes in the cingulate cortex and cerebral cortex surrounding sulci of the familial dogs with seizures (Figs. 9B, 11A). IL-6-positive cells were not found in either the cerebrum of the familial dogs without seizures or control dogs (Fig. 11B). Statistical analysis indicated that the number of IL-6-positive cells was significantly increased in connection with the severity of acute neuronal change (Fig. 12). VEGFR-1-positive

immunolabeling and TNF-α-positive immunolabeling were not detected in GFAP-positive astrocytes (Fig. 7B, 8B).

DISCUSSION

In this study, histopathologic and immunohistochemical examination demonstrated that acute neuronal change, angiogenesis and microglial activation were localized in the cingulate cortex and cerebral cortex surrounding sulci of familial dogs with seizures. The acute neuronal change was thought to be seizure-induced neuronal death because it was not detected in the familial dogs without seizures. Production of VEGF in neurons and glial cells, long and tortuous microvessels, proliferation of vWF-positive vascular endothelial cells, and an increase in the number of microvessels have all been reported to be related to angiogenesis (Rigau et al., 2007; Nodode-Ekane et al., 2010). Morphologic changes in microglia (swollen cell bodies and long processes) and pro-inflammatory cytokine production suggested microglial activation (Avignone et al., 2008). In this study, pro-inflammatory cytokine production was immunohistochemically detected in the cerebrum of familial dogs with seizures. TNF-α-positive immunolabeling was detected in activated microglia. TNF-α has been reported to induce neurotoxicity by down-regulation of astrocytic glutamate transporter 1 (GLT-1) (Carmen et l., 2009) (an important transporter for astrocytic glutamate uptake from the synaptic cleft (Rothstein et al., 1994; Sonnewald et al., 1997), and the induction of

excess glutamate release due to microglial activation in an autocrine manner has been described (Takeuchi et al., 2006). In the cerebrum of familial dogs with seizures, a previous study demonstrated a high concentration of glutamate in the cerebrospinal fluid (Morita et al., 2002), a decrease in the immunopositivity of GLT-1 and excess glutamate immunopositivity in almost the same distribution as that of acute neuronal change and activated microglia (Morita et al., 2005). Glutamate is an excitatory neurotransmitter and excess glutamate is known to induce neurotoxicity, called excitoneurotoxicity (Rajdev et al., 1994). TNF-α, which was induced in the activated microglia, could cause glutamate metabolism dysfunction, leading to neuronal death. IL-6-positive immunolabeling was detected in activated microglia, and also in neurons and astrocytes in the cerebrum of familial dogs with seizures. Neuronal hyper-excitability has been reported to induce neuronal production of IL-6 (Sallmann et al., 2000) and IL-6 has been thought to have both direct and indirect neuroprotective effects against neuronal hyper-excitability (Gradient et al., 1997; Vezzani et al., 2008b; Yamada et al., 1994). However, in the cerebrum of familial dogs with seizures, IL-6-positive cells were observed in almost the same distribution as that of acute neuronal change, and the increase in the number of IL-6-positve cells was related to the severity of acute neuronal change. The increased number of IL-6-positive cells reflected an

increase in the number of IL-6-positive glial cells, because neurons with acute change were negative for IL-6. Overproduction of IL-6 in glial cells has been reported to cause neuronal death (Campbell et al., 1993). In the cerebrum of familial dogs with seizures, production of IL-6 in the glial cells may cause local overproduction of IL-6, resulting in neuronal death. Thus, microglial activation with pro-inflammatory cytokine production was thought to be responsible for the seizure-induced neuronal death in the cerebrum of familial dogs with seizures.

In the cerebrum of familial dogs with seizures, neurons, astrocytes and microglia were immunohistochemically positive for VEGF. Production of VEGF in neurons and astrocytes has been reported to be induced by seizures in human epilepsy and in animal models of epilepsy, and VEGF is thought to contribute to angiogenesis for neuroprotection (van Vliet et al., 2007; Ndode-Ekane et al., 2010). However, in this study, the distribution of the VEGF-positive cells was consistent with that of the activated microglia and the activated microglia were immunohistochemically positive for VEGFR-1. VEGF has been reported to activate microglia via VEGFR-1 and induce an inflammatory response (Croll et al., 2004; Forstreuter et al., 2002). In addition, TNF-α and IL-6 have been reported to be induced by VEGF via VEGFR-1 in macrophages and monocytes (Yoo et al., 2005). Recently, monocytes in the bloodstream have been

thought to enter the brain during embryonic development and differentiate into microglia displaying many cell surface antigens found in macrophages (Kim et al., 2005). In the cerebrum of the familial dogs with seizures, VEGF produced in neurons and astrocytes could activate microglia and induce overproduction of TNF-α and IL-6 in microglia. Moreover, recent evidence suggests that microglia are not only responsive to, but also sources of VEGF (Ryu et al., 2009). The activated microglia, which were immunohistochemically positive for VEGF, may induce further microglial activation in the cerebrum of familial dogs with seizures.

Thus, anigogenesis and microglial activation was thought to be related to seizure-induced neuronal death. Present study can't provide evidence about whether angiogenesis and microglial activation are a cause of seizure-induced neuronal death or a subsequent event of seizure-induced neuronal death. However, VEGF-positive cells and activated microglia were detected not only in the areas of acute neurona change but also in the areas surrounding acute neuronal change. The distribution suggested that angiogenesis and microglial activation can accelerate seizure-induce neuronal death and expand the lesions. VEGF-induced microglial activation with pro-inflammatory cytokine production is thought to play a critical role in neuronal death. Further investigation into how microglia are activated and how activated microglia damage

neurons in an epileptic brain after a seizure is required. These investigations may lead to novel therapeutic approaches against the progression of epilepsy.

FIGURES AND FIGURE LEGENDS

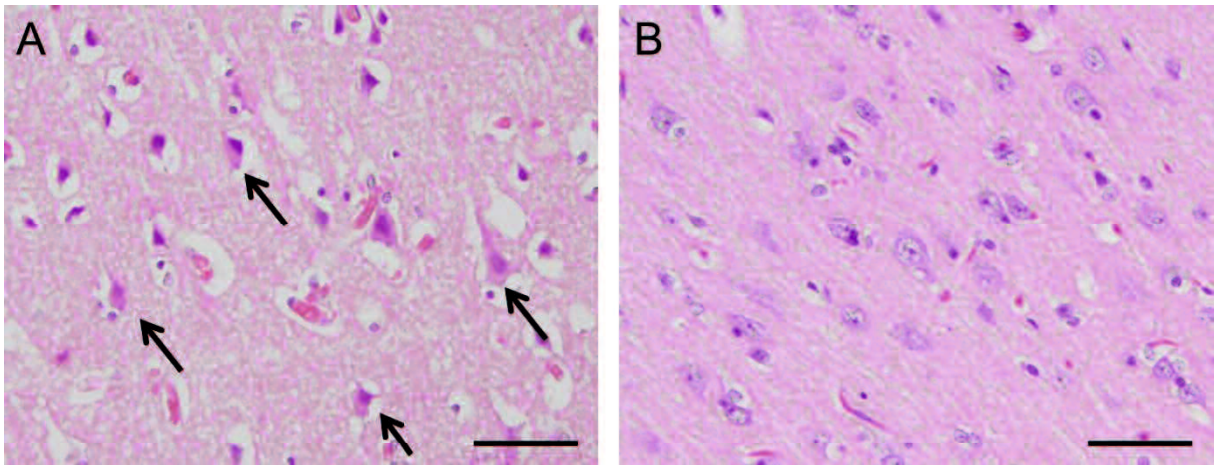

Fig. 1 Representative images of the cerebrum (cingulate cortex) in a familial dog with seizures (No. 3) and a familial dog without seizures (No. 7). Acute neuronal change (arrows) is observed in a familial dog with seizures (A). No significant changes were observed in a familial dog without seizures (B). H&E stain; bars = 50 μm.

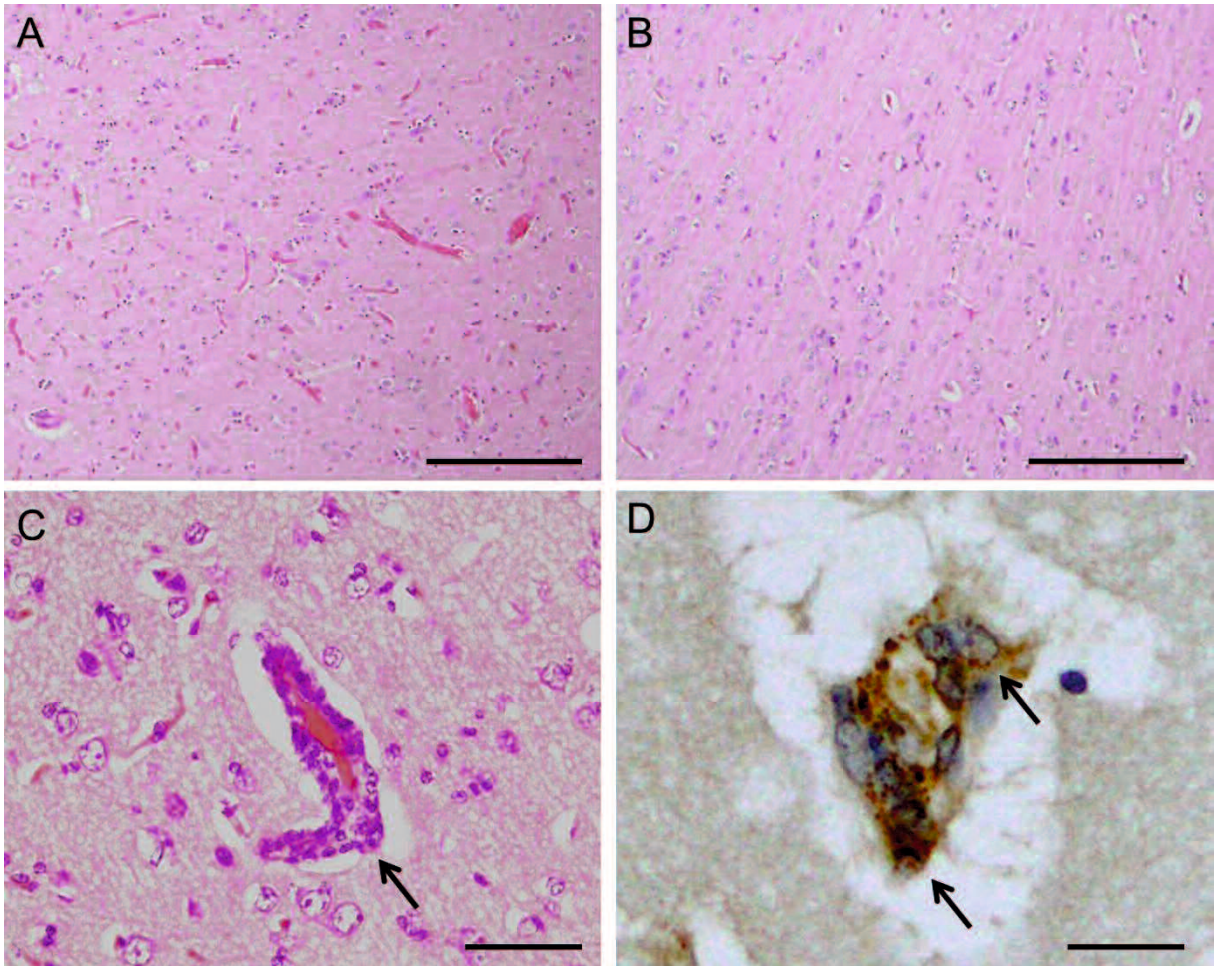

Fig. 2 Representative images of the cerebrum (cingulate cortex) in a familial dog with seizures (No. 1) and a familial dog without seizures (No. 8). Comparing a familial dog with seizures (A) and a familial dog without seizures (B), microvessels appeared longer and more tortuous in a familial dog with seizures. Oval to flat cells surround the microvessel (C), and these cells are positive for vWF (D, arrows) in a familial dog with seizures. H&E stain (A-C) and labeled streptavidin-biotin for vWF (D); bars = 200 μm (A, B), 50 μm (C), 20 μm (D).

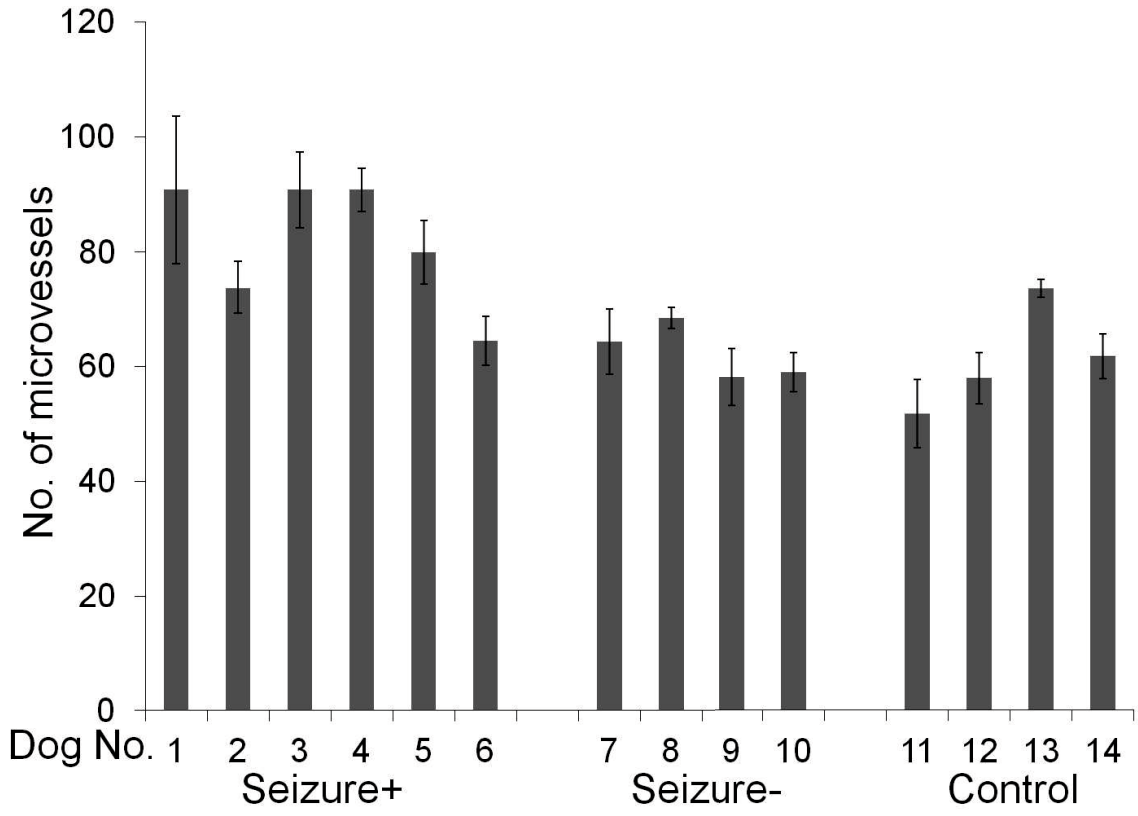

Fig. 3 Number of microvessels in the cingulate cortex. Comparing with the familial dogs without seizures and control dogs, the number was significantly increased in the familial dogs with seizures. There are no significant differences in the familial dogs without seizures and control dogs. *P<0.05.

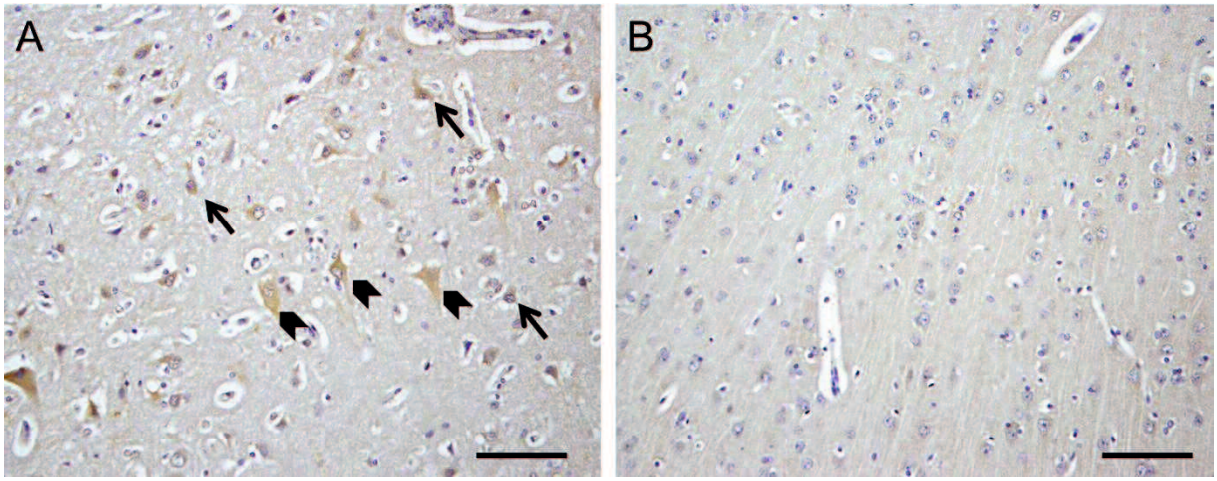

Fig. 4 Representative images of cerebrum (cingulate cortex) in a familial dog with seizures (No. 2) and a familial dog without seizures (No. 10). Some glial cells (arrows) and neurons (arrowheads) are positive for VEGF in a familial dog with seizures (A). There are no VEGF-positive cells in a familial dog without seizures (B). Labeled streptavidin-biotin for VEG

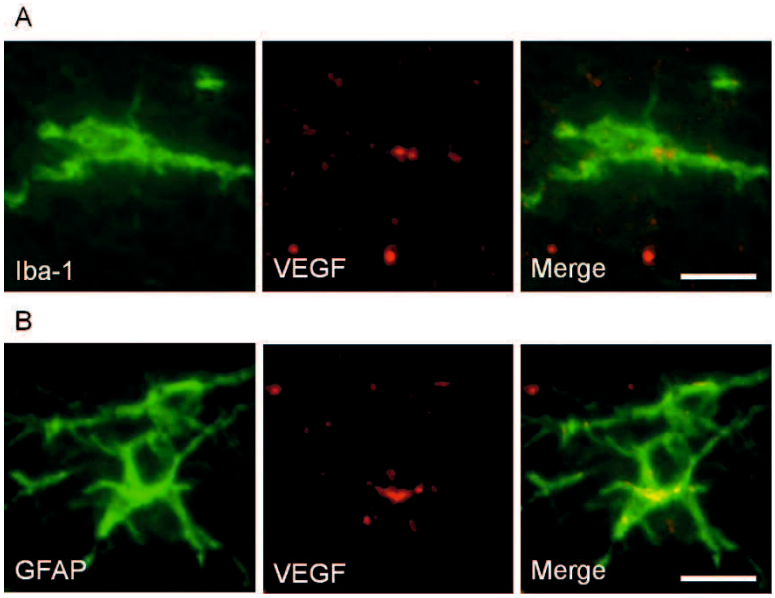

Fig. 5 Representative images of cerebrum (cingulate cortex) in a familial dog with seizures (No.1). VEGF-positive signals (red signals) are detected in both Iba-1-positive microglia (A, green signals) and GFAP-positive astrocyte (B, green signals). Double-label immunofluorescence; bars = 30μm.

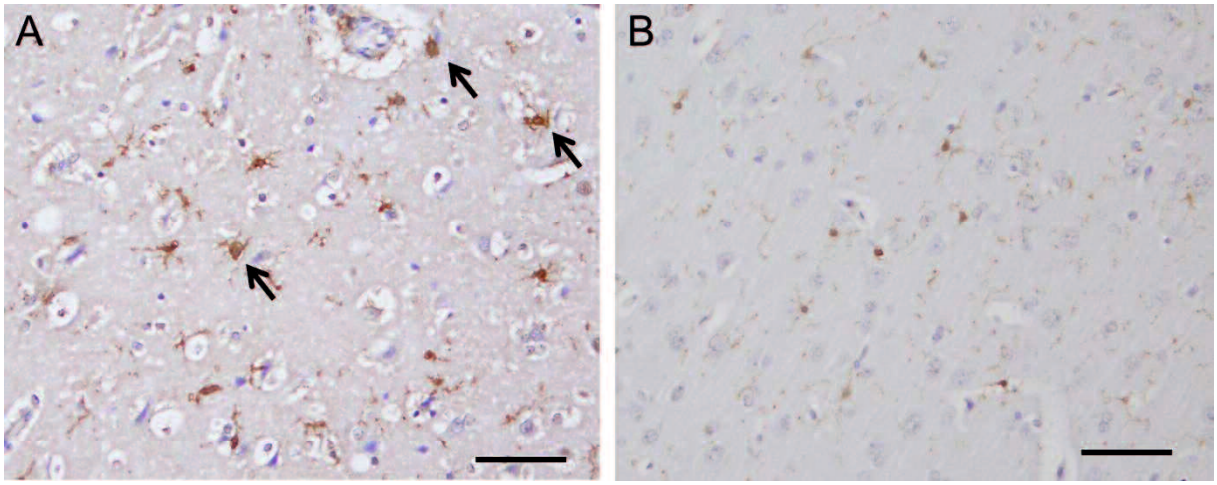

Fig. 6 Representative images of cerebrum (cingulate cortex) in a familial dog with seizures (No. 2) and a familial dog without seizures (No. 8). Comparing a familial dog with seizures (A) and the familial dogs without seizures (B), Iba-1-positive microglia increase and have swollen cell bodies and longer processes in the familial dogs with seizures (arrows). Labeled streptavidin-biotin for Iba-1; bars = 50 μm.

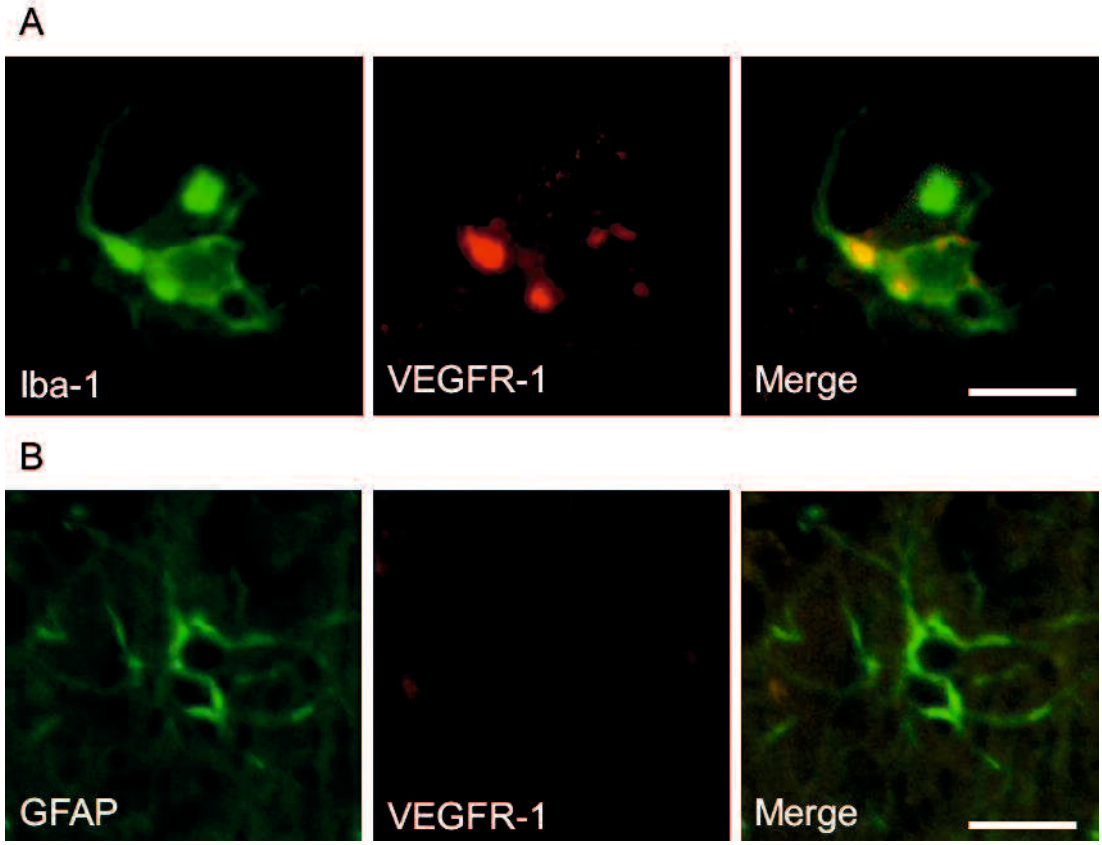

Fig. 7 Representative images of cerebrum (cingulate cortex) in a familial dog with seizures (No.5).VEGFR-1-positive signals (red signals) are detected in Iba-1-positive microglia (A, green signals), and not detected in GFAP-positive astrocyte (B, green signals). Double-label immunofluorescence; bars = 30μm.

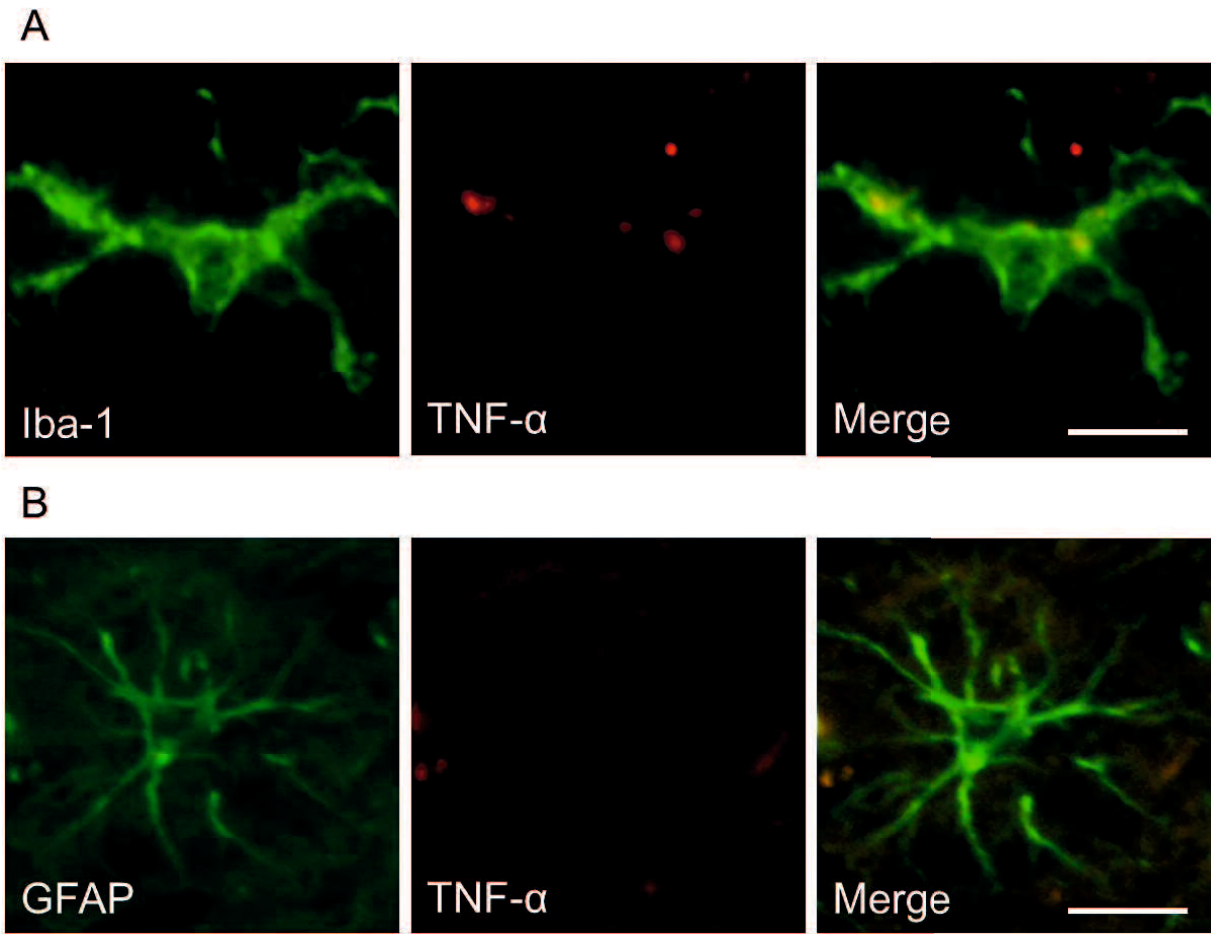

Fig. 8 Representative images of cerebrum (cingulate cortex) in a familial dog with seizures (No. 2). TNF-α-positive signals (red signals) are detected in Iba-1-positive microglia (A, green signals), and not detected in GFAP-positive astrocyte (B, green signals). Double-label immunofluorescence; bars = 30μm.

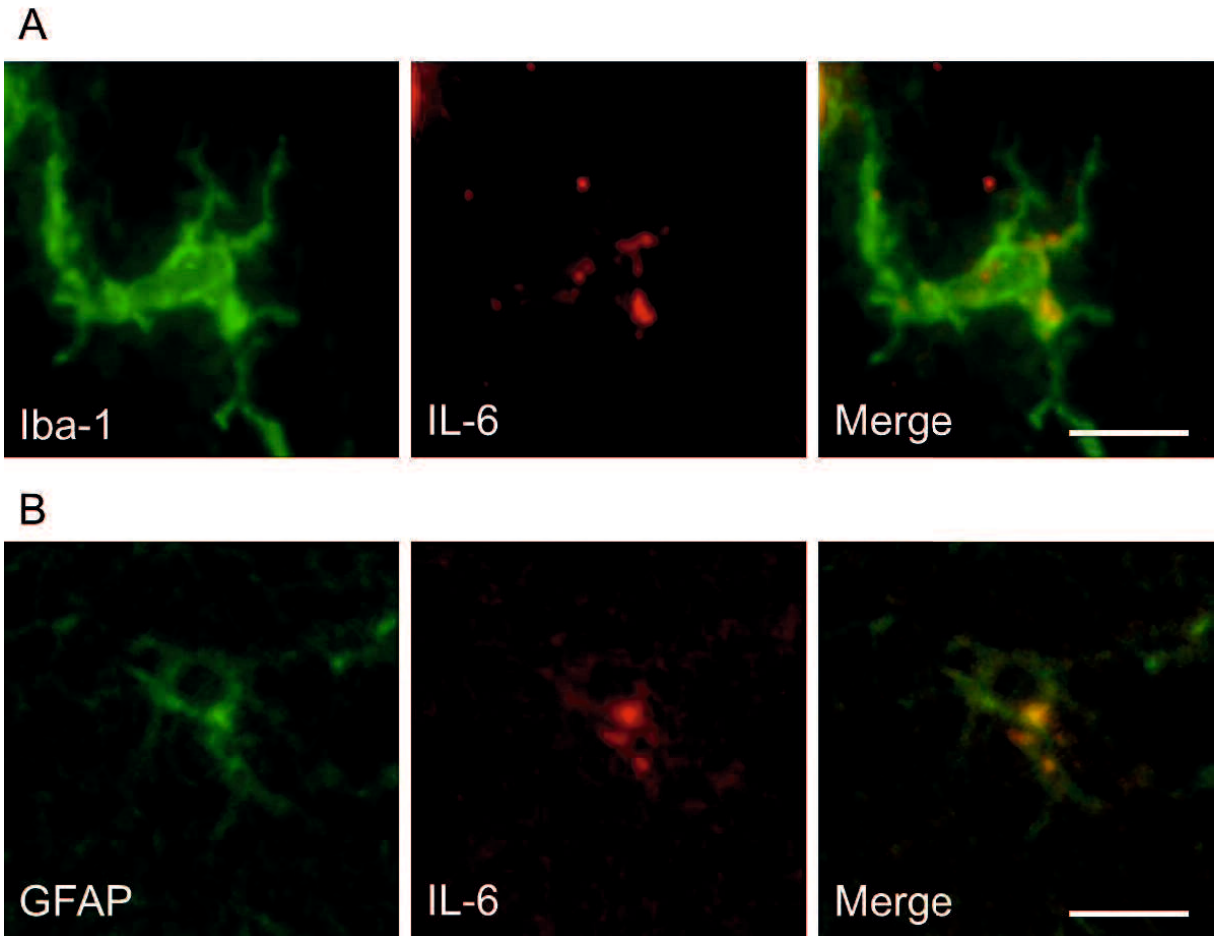

Fig. 9 Representative images of cerebrum (cingulate cortex) in a familial dog with seizures (No. 1). IL-6-positive signals (red signals) are detected in Iba-1-positive microglia (A, green signals) and GFAP-positive astrocyte (B, green signals). Bars = 30μm.

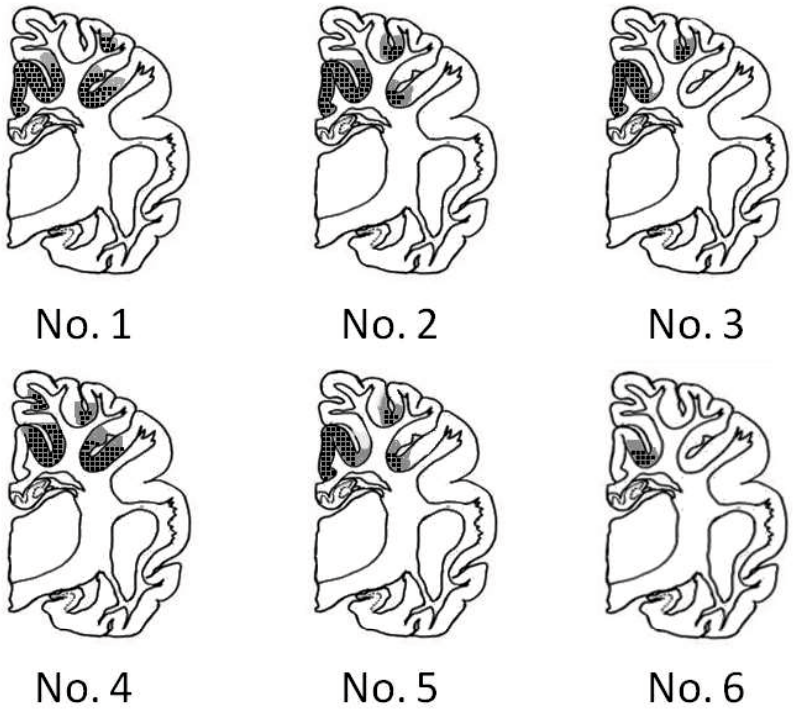

Fig. 10 Distribution of the neurons with acute change (black dot) and distribution of VEGF-positive cells and activated microglia (gray color) at the coronal level of corpus mamillare in the familial dogs with seizures. The distribution of VEGF-positive cells and activated microglia was similar to that of neurons with acute change, in addition, VEGH-positive cells and activated microglia were also observed in the areas surrounding neurons with acute change.

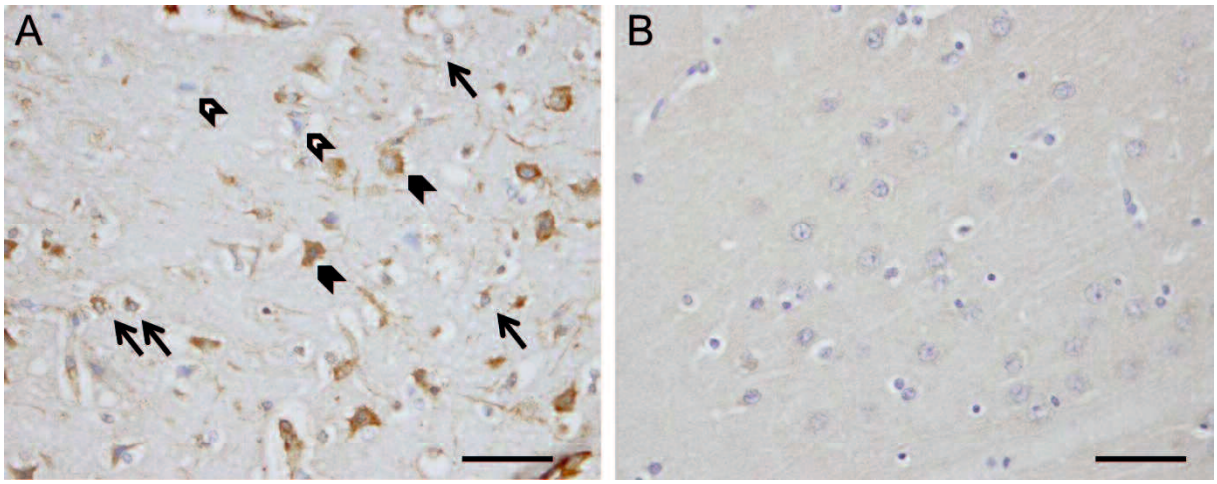

Fig. 11 Representative images of cerebrum (cingulate cortex) in a familial dog with seizures (No. 2) and a familial dog without seizures (No. 10). Neurons (black arrowheads) and glial cells (arrows) are positive for IL-6, but neurons with acute change (white arrowheads) are negative for IL-6 in a familial dog with seizures (A). There are no IL-6-positive cells in the cingulate cortex of the familial dogs without seizures (B). Labeled streptavidin-biotin for IL-6; bars = 50 μm.

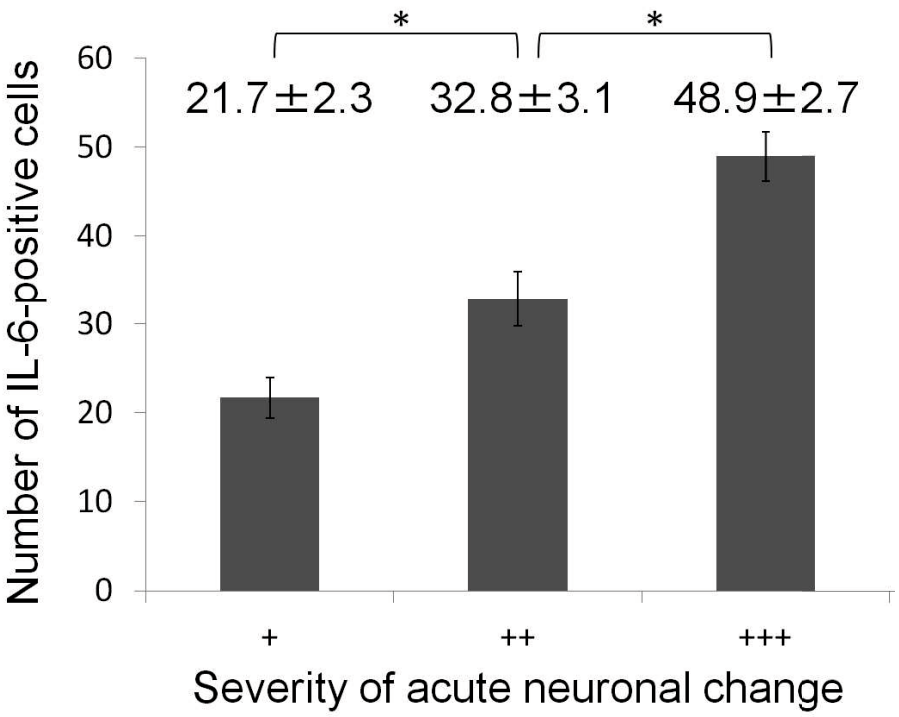

Fig. 12 Number of IL-6-positive cells in each severity of acute neuronal change in the familial dogs with seizures. Number of IL-6-positive cells is significantly increased in the area of more severe acute neuronal change. *P<0.05.

TABLES

Table. 1 Primary antibodies used for immunohistochemistry

Antibody	Source	Dilution	Incubation	Supplier
GFAP	Rabbit polyclonal	1:100	10 min in microwave	Dako, Glostrup, Denmark
Iba-1	Rabbit polyclonal	1:400	10 min in microwave	Wako Chemicals, Richmond, USA
IL-6	Mouse monoclonal	1:100	overnight at 4 °C	Santa Cruz, California, USA
TNF-α	Mouse monoclonal	1:300	overnight at 4 °C	Santa Cruz, California, USA
VEGF	Mouse monoclonal	1:100	overnight at 4 °C	Abcam, Tokyo, Japan
vWF	Rabbit polyclonal	1:100	10 min in microwave	Dako, Glostrup, Denmark
VEGFR-1	Mouse monoclonal	1:100	overnight at 4 °C	Abcam, Tokyo, Japan

Abbreviations: GFAP, glial fibrillary acidic protein; IL-6, interleukin 6; TNF-α, tumor necrosis factor alpha; VEGF, vascular endothelial growth factor; vWF, von Willebrand factor; VEGFR-1, vascular endothelial growth factor receptor 1.

CHAPTER 2

Glutamate transporter 1 downregulation correlates with thalamic neuronal death following kainic acid-induced status epilepticus in rat

ABSTRACT

Recurrent seizures without interictal resumption (status epilepticus) have been reported to induce neuronal death in the midline thalamic region that has functional roles in memory and decision-making; however, the pathogenesis underlying status epilepticus-induced thalamic neuronal death is yet to be determined. We performed histological and immunohistochemical studies as well as cerebral blood flow measurement using 4.7 tesla magnetic resonance imaging spectrometer on midline thalamic region in Sprague–Dawley rats (n=67, male, 7 weeks after birth, body weight 250 - 300 g) treated with intraperitoneal injection of kainic acid (10 mg/kg) to induce status epilepticus (n=47) or normal saline solution (n=20). Histological study using paraffin-embedded specimen revealed neuronal death showing ischemic-like changes and Fluoro-Jade C -positivity with calcium deposition in the midline thalamic region of epileptic rats. The distribution of neuronal death was associated with focal loss of immunoreactivity for glutamate transporter 1 (GLT-1), stronger immunoreaction for glutamate and increase in number of Iba-1-positive microglial cells showing swollen cytoplasm and long processes. Double immunofluorescence study demonstarted co-expression of interleukin-1 beta (IL-1β) and inducible nitric oxide synthase (iNOS)

within microglial cells, and loss of GLT-1-immunoreactivity in reactive astrocytes. These microglial alterations and astrocytic GLT-1-downregulation were also observed in tissue without obvious neuronal death in kainic acid-treated rats. These results suggest the possible role of glutamate excitotoxicity in neuronal death in the midline thalamic region following kainic acid-induced status epilepticus due to astrocytic GLT-1 downregulation following microglial activation showing upregulation of IL-1β and iNOS.

INTRODUCTION

Epilepsy is a chronic neurological condition characterized by recurrent seizures due to neuronal hyperexcitation (Blume et al., 2001). The prevalence of epilepsy in general has been reported between 4 to 10 per 1,000 persons (Sander et al., 2003). Approximately 30 percent of epilepsy patients do not have seizure remission despite appropriate medical treatment (Kwan et al., 2000). Patients with intractable epilepsy also suffer from sequellae of brain dysfunctions including memory loss, language impairment, depression and olfactory dysfunction (Alessio et al., 2006; Jacek et al., 2007; Kanner et al., 2011). Recurrent seizures without interictal resumption or "status epilepticus" is known to induce neuronal death in the limbic system (Fujikawa et al., 2000; Meldrum et al., 1993).

Classical experimental studies have shown that systemic injection of kainic acid, a glutamate receptor agonist, in rodents induces seizures and epileptiform discharges in the hippocampus that propagate to other limbic structures (Pinheiro et al., 2006), and neuronal death in the cornu ammonis of the hippocampal formation, piriform cortex, and specific nuclei of the thalamus (Gayoso et al., 2003). Status epilepticus-induced neuronal death is frequently observed in the midline region, particularly the

mediodorsal nucleus (MD) and nucleus reuniens (Re) in the thalamus (Gayoso et al., 2003). The MD and Re are thought to play functional roles in memory, olfactory perception and decision-making in human and animals (McKenna et al., 2004; Tham et al., 2009; Vertes et al., 2002). Magnetic resonance imaging (MRI) analyses have demonstrated thalamic volume reduction in epilepsy patients (Helms et al., 2006; Natsume et al., 2003), however, there are few reports on the pathogenesis of status epilepticus-induced neuronal death in the thalamus (Ingvar et al., 1988). We performed histological and immunohistochemical studies as well as cerebral blood flow measurement using 4.7 tesla MRI spectrometer on midline thalamic region in kainic acid-induced status epilepticus in Sprague–Dawley rats to investigate the pathogenesis of status epilepticus-induced neuronal death in the thalamus, focusing on glutamate transporter 1 (GLT-1) downregulation and microglial activation, that are recently reported in the epileptic brains (Najjar et al., 2011; Proper et al., 2002).

MATERIALS AND METHODS

Animals

Sixty-seven Sprague–Dawley rats (7 weeks old, male, body weight 250 - 300 g, CLEA Japan Inc., Tokyo, Japan) were used in this study. Animals were maintained at a constant temperature (25°C) and humidity (55 - 70%) under a 12/12 h light/dark cycle with free access to food and water. The study was carried out with the approval of the Animal Research Committee, in accordance with the guidelines for animal experiment of the Faculty of Agriculture, Tottori University.

Induction of status epilepticus

Forty-seven rats were subjected to intraperitoneal injection of kainic acid (5 mg/ml in saline, 10 mg/kg; Sigma-Aldrich, St. Louis, USA) to induce status epilepticus, and 20 animals were treated with the same volume of normal saline solution (Otsuka Seiyaku, Tokyo, Japan) as controls. The induction of status epilepticus was judged using the behavioral scale proposed by Zhang and colleagues (Zhang et al., 1997). In brief, the epileptic convulsion profile of rats was classified according to 6 distinct stages characterized by; stage 1, immobilization, staring, mouth and facial movements; stage 2,

wet dog shakes; stage 3, forelimb clonus and head nodding; stage 4, rearing; stage 5, rearing and falling; and stage 6, jumping and circling. Kainic acid-treated rats that exhibited at least stage 4 convulsions were judged as having status epilepticus in this study. The rats having status epilepticus (n=27) were kept for 0 day (5 hours after kainic acid injection; n=5), 7 (n=9), 14 (n=8) and 28 days (n=5). The rats without status epilepticus (n=20) and saline-treated controls (n=20) were also kept in the same manner (n=5 for each maintenance period). During the maintenance period, the rats having status epilepticus were monitored by a video camcorder for 24 hours a day.

Cerebral blood flow measurement

Cerebral blood flow (CBF) measurement was performed on 4 rats having status epilepticus and 4 rats without status epilepticus, by means of continuous arterial spin labeling (CASL) method with a labeling neck coil (Rapid Biomedical GmbH, Rimpar, Germany) using a 4.7 tesla MRI spectrometer (Unity Inova, Varian Inc., California, USA). The rats which exhibited status epilepticus (rearing) were anesthetized and set in the bore. Animals were anesthetized with isoflurane (0.5–1.5% with a 1:9 ratio of oxygen and room air) throughout the experiment. CBF was measured on the coronal plane including MD and Re determined by referencing to the T2-weighted images and a

stereotaxic atlas. Magnetic resonance images for CASL were acquired using a gradient echo sequence with the following characteristics: response time, 8 ms; echo time, 4 ms; field of view, 25 mm; matrix size, 64 x 64. A post delay of 400 ms was used for CASL CBF imaging. CASL CBF was calculated in accordance with the previous reports (Nakamura et al., 2008). The kainic acid-treated rats without status epilepticus were subjected to CBF measurement 90 min after the drug injection. The average of CASL CBF in each rat was measured in the areas of interest including MD and Re. Mann–Whitney test was used for statistical analysis of the data between rats with and without status epilepticus.

Histological and immunohistochemical studies

Under deep anesthesia with intraperitoneal injection of sodium pentobarbital (64.8 mg/kg, Kyoritsu Seiyaku, Tokyo, Japan), brains were removed and fixed in 10% neutral phosphate-buffered formalin for 72 hours, and cut coronally with 2 mm intervals. The specimens were embedded in paraffin wax and sectioned at 4 μm for hematoxylin and eosin, Alizarin Red S (Kanto Chemical Co., Inc., Tokyo, Japan) (Dahl, 1952), and Fluoro-Jade C (Chemicon, Temecula, CA, USA) stainings as well as immunohistochemical studies using the following primary antibodies; Iba-1 (mouse

monoclonal, clone 1022-5, dilution 1:200; Abcam, Tokyo, Japan), glial fibrillary acidic protein (GFAP; mouse monoclonal, clone 6F2, dilution 1:200; Dako, Glostrup, Denmark), GLT-1 (rabbit polyclonal, dilution 1:500; Wako Chemicals, Richmond, USA), and glutamate (mouse monoclonal, clone GLU-4, dilution 1:400; Sigma-Aldrich). After deparaffinization, the sections were subjected to microwave irradiation in sodium citrate buffer (pH 6.0) for 20 min at 98°C in a microwave processor (MI-77, Azumaya inc., Tokyo, Japan). Subsequently, after blocking endogenous peroxidase activity with 3% hydrogen peroxide for 15 min, sections were preincubated with 10% normal goat serum for 5 min in the microwave processor. Then, the sections were incubated with primary antibodies for overnight at 4°C for glutamate, and for 10 min under continuous microwave irradiation for Iba-1, GFAP and GLT-1. Sections were incubated with appropriate goat anti-rabbit or anti-mouse immunoglobulins conjugated to peroxidase labeled-dextran polymer (EnVision+ System-HRP, Dako, Carpinteria, CA, USA) for 30 min at room temperature (approx. 20°C). The immunoreaction was visualized using 3,3′-diaminobenzidine tetrahydrochloride (Dako, Carpinteria, CA, USA). Sections were finally counterstained with hematoxylin. For double immunofluorescence studies, sections were incubated with a mouse monoclonal anti-Iba-1 antibody or a mouse monoclonal anti-GFAP antibody for 10 min in the

microwave processor, followed by incubation with an Alexa Fluor 555-conjugated donkey anti-mouse IgG antibody (dilution 1:200; Life Technologies, Carlsbad, USA) for 1 hour at room temperature. Sections were then incubated with rabbit polyclonal antibodies for GLT-1, interleukin-1 beta (IL-1β; dilution 1:50; Santa Cruz, California, USA), or inducible nitric oxide synthase (iNOS; dilution 1:100; Abcam) for overnight at 4°C, followed by incubation with an Alexa Fluor 488-conjugated goat anti-rabbit IgG antibody (dilution 1:200; Life Technologies) for 1 hour at room temperature. Sections were mounted in plain 80% Tris-buffered glycerol and observed under a fluorescence microscope (AX-70, Olympus Corporation, Tokyo, Japan). Appropriate positive controls were carried out by omission of the primary antibodies replacing with phosphate-buffered saline.

Morphometry and statistical analysis

For morphometry and statistical analysis, the sections that include MD and Re were selected based on the stereotaxic atlas of the rat brain (Paxions et al., 1986), and the areas of MD and Re were defined by the coordinate system (x, y). Y-axis was set parallel to the fissura longitudinalis cerebri, and X-axis intersected at a right angle with the Y-axis. The point (0, 0) was located at the midline lower end of the section. The

rectangles made from the following 4 points were defined in the area of MD: (-1.2 mm, 5.1 mm), (-1.2 mm, 4.4 mm), (1.2 mm, 4.4 mm) and (1.2 mm, 5.1 mm). Also, the rectangles made from the following 4 points were defined in the area of Re: (-0.8 mm, 3.4 mm), (-0.8 mm, 3.2 mm), (0.8 mm, 3.2 mm) and (0.8 mm, 3.4 mm). All bright-field photographs were taken by the digital camera (DP-21, Olympus, Tokyo, Japan) attached to the light microscope (BX-51, Olympus).

The percentage of GLT-1-immunoreactive area (GLT-1-IRA%) was calculated in each rat by means of computer-assisted image analysis using Image-Pro® (Nippon Roper, Tokyo, Japan) software using the digital images taken with x10 objective lens (1.3 mm^2).

The total number of Iba-1-positive microglia and the percentage of morphologically activated microglia were manually counted and calculated in the MD and Re of each rat using the 5 non-overlapping digital images in each nucleus taken with x40 objective lens (0.1 mm^2). The average number of microglia per 1 mm^2 was counted in each rat, and semiquantitative evaluation was performed according to the following criteria; i.e., ‘mild increase’ when more than 200 but less than 400 microglial cells per 1 mm^2 were observed, and ‘marked increase’ when the number was 400 or more.

For each group (rats having status epilepticus, rats without status epilepticus and controls), the mean values of the GLT-1-IRA% and the number of Iba-1-positive microglia at each time point were statistically compared by Kruskal–Wallis test. At each time point, the difference among the rats having status epilepticus, the rats without status epilepticus, and controls was analyzed using the analysis of variance followed by a post hoc Scheffe's test for multiple comparisons. The statistical difference was considered to be significant when the *p* value was less than 0.05.

The number of GFAP-positive reactive astrocytes (having swollen cytoplasm, thick short processes, and occasional multiple nuclei) were counted in MD and Re in each rat, and judged as 'mild increase' when the number of reactive astrocytes was less than 15, and 'marked increase' for the number of 15 or more.

RESULTS

Induction of status epilepticus

Twenty-seven of 47 rats (57.4%) with kainic acid injection started to show wet dog shakes at 30 to 60 min after treatment. Within 180 min after injection, they showed recurrent rearing (classified as stage 4 of Zhang's scale). A rearing was maintained for 30-180 sec and sometimes lead to falling (stage 5). Rearing completely disappeared within 5 hours after injection. 27 rats having status epilepticus were divided and kept for 0 day (5 hours after kainic acid injection, n=5), 7 (n=9), 14 (n=8) and 28 days (n=5). During the maintenance period, recurrent spontaneous seizures were absent as long as the observation through video camcorder. No rats died during the maintenance period. Other 20 rats with kainic acid injection and saline-treated controls did not show any behavioral alterations.

CBF measurement

The means and standard deviation of CASL CBF in the midline thalamic region were 76.3±17.9 (4 rats having status epilepticus) and 93.3±7.5 (4 rats without status

epilepticus). There were no statistically significant differences in the CBF measurement data between them (Fig. 1).

Histological findings (Table 1)

In the brains of rat showing status epilepticus (5 rats in day 7, 5 rats in day 14 and 5 rats in day 28), both intracellular and extracellular calcifications were observed in MD and Re (Fig. 2A). These calcifications were strongly positive for Alizarin Red S staining. Within the lesions, neurons exhibited ischemic-like changes showing shrunken eosinophilic cytoplasms and karyolysis (Fig. 2B), and Fluoro-Jade C staining-positive degenerating neurons were observed. On the other hands, there were no significant histological changes in all rats without status epilepticus and control animals. Based on these findings, status epilepticus-induced neuronal death in the MD and Re was confirmed.

Immunohistochemical findings (Table 1)

Glutamate: GLT-1 immunoreactivity was focally decreased in MD and Re of rats having status epilepticus (Figs. 3A, B). The focal loss of GLT-1 immunoreactivity was colocalized with the lesion showing neuronal death. In addition, there was a mosaic-like

loss of GLT-1 immunoreactivity in MD and Re of rat having status epilepticus without obvious neuronal death (2 rats in day 7 and 3 rats in day 14). Other rats having status epilepticus did not show any immunohistochemical difference compared with the rats without status epilepticus and controls, showing diffuse GLT-1 immunopositivity in the cytoplasm and process of astrocytes. Within the lesions showing neuronal death, there was a focal glutamate immunopositivity in the neuropil (Figs. 3C, D). No glutamate immunoreactivity was detected in other rats having status epilepticus, and rats without status epilepticus as well as controls.

Temporal decrease in the GLT-1-IRA% was observed in both MD and Re of rats having status epilepticus ($p<0.05$). Significant decrease in GLT-1-IRA% was observed ($p<0.05$) in MD and Re of rats having status epilepticus compared with the rats without status epilepticus and controls at day 14 and 28 (Fig. 4). There was no significant difference in GLT-1-IRA% between rats without status epilepticus and controls at each time point.

Microglia: Increased number of Iba-1-positive microglia was a characteristic finding in MD and Re of rats having status epilepticus, except day 0 group (Fig. 5A). In addition, Iba-1-positive microglia exhibited an activated shape (swollen cell bodies and long

processes) (Fig. 5B). Double immunofluorescence revealed extensive IL-1β- and iNOS-immunolabelings in Iba-1-positive microglial cells of activated shape (Fig. 6). Temporal increase in the number of Iba-1-positive microglia was observed in both MD and Re of rats having status epilepticus ($p<0.05$). Significant increase in number of microglia was statistically confirmed ($p<0.05$) at all time points except day 0, in MD and Re of rats having status epilepticus compared with the rats without status epilepticus and controls (Fig. 7).

Astrocytes: Increased number of GFAP-positive astrocytes was observed in MD and Re of rats having status epilepticus, particularly in the peri-lesional area (Fig. 8A). In the center of the lesion, reactive astrocytes showing swollen cytoplasm, thick short processes, and occasional multiple nuclei (Fig. 8B) were observed only in rats having status epilepticus (5 rats in day 7, 8 rats in day 14 and 5 rats in day 28). Double immunofluorescence did not show GLT-1-, IL-1β and iNOS immunolabelings in these reactive astrocytes.

DISCUSSION

In this study, status epilepticus-induced neuronal death was indicated by the morphological (ischemic-like) changes of neurons and Fluoro-Jade C staining in the midline thalamic region, particularly in the MD and Re. These findings coincide with a previous report (Gayoso et al., 2003). Although seizure-induced neuronal injury was originally thought to be “ischemic injury”, Meldrum and colleagues demonstrated non-ischemic, seizure activity-induced irreversible neuronal injury (Meldrum et al., 1992). CBF measurement in our study also suggested no CBF alterations immediately after status epilepticus. Recent studies have supported the concept that the thalamus, particularly the midline thalamic region, is a part of the epileptic circuits of temporal lobe epilepsy (Bertram, 2012). Neuronal death in the midline thalamic region of kainic acid-treated rat might be triggered by status epilepticus.

Decrease in GLT-1 immunopositive area and microglial activation were characteristic findings within the lesion. In addition, time-dependent decrease in GLT-1 immunopositive area and microglial activation were observed after status epilepticus. These changes, together with the fact that GLT-1 downregulation were also observed in

the lesions without neuronal death (2 rats in day 7 and 3 rats in day 14), suggest the important preceding mechanism for inducing neuronal death.

The decrease in GLT-1 immunopositive area observed in the present study was largely attributable to the astrocytic GLT-1 downregulation. Immunohistochemically, GFAP-positive, but GLT-1-negative, reactive astrocytes were present in the lesion. GLT-1 is a transporter that is important for astrocytic glutamate uptake in synaptic clefts and expressed in astrocytic foot processes (Anderson et al., 2000). The lesion showing neuronal death and focal decrease in GLT-1 immunopositive area was always associated with a strong glutamate immunoreactivity in the neuropil, while no glutamate immunopositivity was observed in the lesion without apparent neuronal death. These findings suggest that an excessive glutamate accumulation in the synaptic cleft due to astrocytic GLT-1 downregulation resulted in excitotoxic neuronal death (Anderson et al., 2000; Rodríguez et al., 2000). Recent studies have shown that GLT-1 is crucial for neuronal survival (Rao et al., 2001). Futhermore, neuronal death in MD and Re was always associated with calcium deposition as revealed by Alizarin Red S staining. Excess glutamate stimulates its receptors and leads to neuronal hyperexcitation because of intracellular calcium-ion overload (Choi et al., 1988). For this reason, it has been proposed that neuronal death caused by glutamate excitotoxicity is associated with

intracellular and extracellular calcification (calcium deposition) (Gayoso et al., 2003; Rodríguez et al., 2000).Thus, the downregulation of astrocytic GLT-1 resulting in glutamate excitotoxicity was considered as a cause of status epilepticus-induced neuronal death in MD and Re of kainic acid-treated rats. GLT-1 downregulation has been reported in the hippocampus of both human epilepsy patients and animal models of epilepsy (Proper et al., 2002; Ueda et al., 2001). Furthermore, increased levels of glutamate in the thalamus and atrophy of this brain structure have been reported in epileptic patients (Helms et al., 2006; Natsume et al., 2003). Kainic acid is an agonist of glutamate receptors and has excitotoxicity (Pinheiro et al., 2006). However, in this study, there were no neuronal death and other significant changes in the brains of all rats without status epilepticus despite the kainic acid injection.

Another characteristic finding in the lesions of MD and Re was microglial activation. The increased number of Iba-1-positive microglia and morphological changes in microglia (swollen cell bodies and long processes) as well as upregulation of IL-1β and iNOS indicate microglial activation (Avignone et al., 2008). And these changes preceded the decrease in GLT-1 immunopositive area (as it appeared in 2 rats of day 7). Recent studies have shown that astrocytic GLT-1 downregulation is mediated by IL-1β and nitric oxide (synthesized by iNOS) (Yamada et al., 2006; Prow et al.,

2008). Accordingly microglial activation might cause astrocytic GLT-1 downregulation in the midline thalamic region of kainic acid-treated rats. Although, IL-1β and nitric oxide have been reported to have direct neurotoxicity, including excitotoxicity (Brown et al., 2010; Lau et al., 2010; Rijkers et al., 2009), no neuronal death was detected in the MD and Re of 5 rats having status epilepticus, despite the presence of activated microglia with IL-1β and iNOS expression. A growing number of evidence suggests that microglial activation is induced by status epilepticus, and a purinergic stimulus by adenosine triphosphate (ATP) is thought to be important for the microglial activation (Avignone et al., 2008; Shapiro et al., 2008; Somera-Molina et al., 2009). Neuronal hyperexcitation has been reported to be associated with astrocytic ATP release, which can induce microglial activation and IL-1β release (Färber et al., 2006; Schipke et al., 2002; Seifert et al., 2010). As described above, the midline thalamic region is reported to be involved in epileptic circuits. Although we were able to show few evidences, neuronal hyperexcitation associated with astrocytic ATP release might trigger microglial activation in the midline thalamic region during status epilepticus.

In conclusion, this study demonstrated the presence of status epilepticus-induced neuronal death that seemed to be caused by glutamate excitotoxicity. Histological and immunohistochemical findings suggested that microglial activation associated with IL-

1β and iNOS expressions was responsible for astrocytic GLT-1 downregulation, resulting in glutamate excitotoxicity

FIGURES AND FIGURE LEGENDS

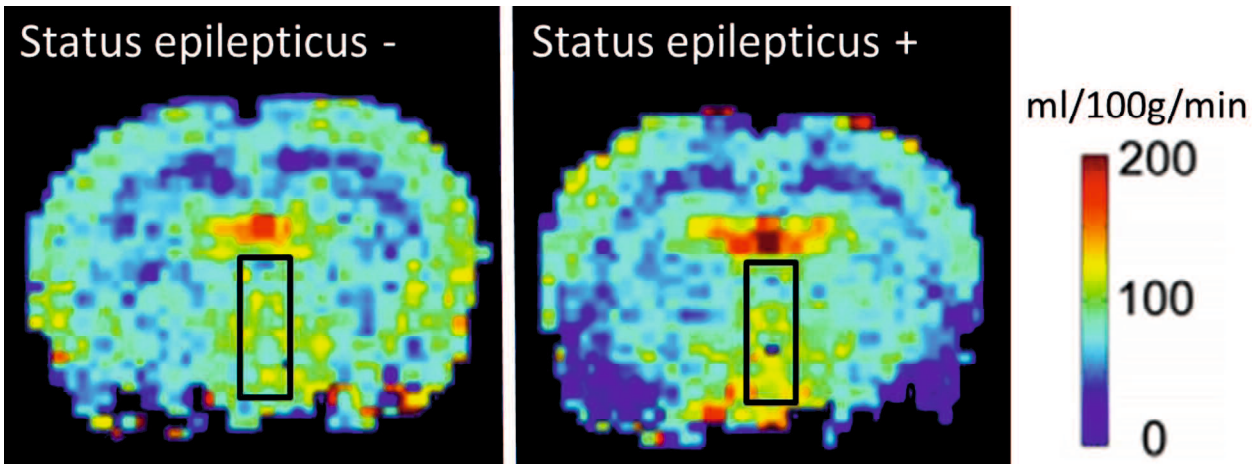

Figure 1. Representative image of cerebral blood flow measurements. There are no significant differences in the CBF images in the midline thalamic region (in the black frames) between the rats having status epilepticus and the rats without status epilepticus.

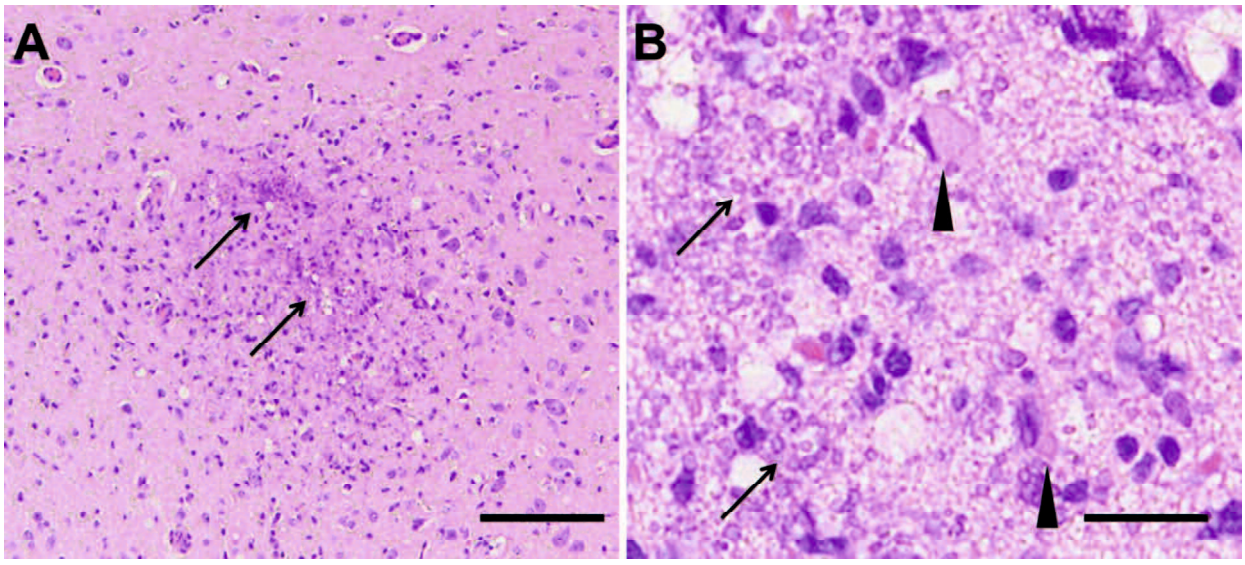

Figure 2. Neuronal death with calcification in the nucleus reuniens of rat having status epilepticus. Extracellular calcification (A, B, arrows) and neurons exhibiting ischemic-like changes (shrunken eosinophilic cytoplasm and karyolysis are present in the lesion (B, arrowheads). Hematoxylin and eosin staining. Bars, 100 μm (A) and 20 μm (B).

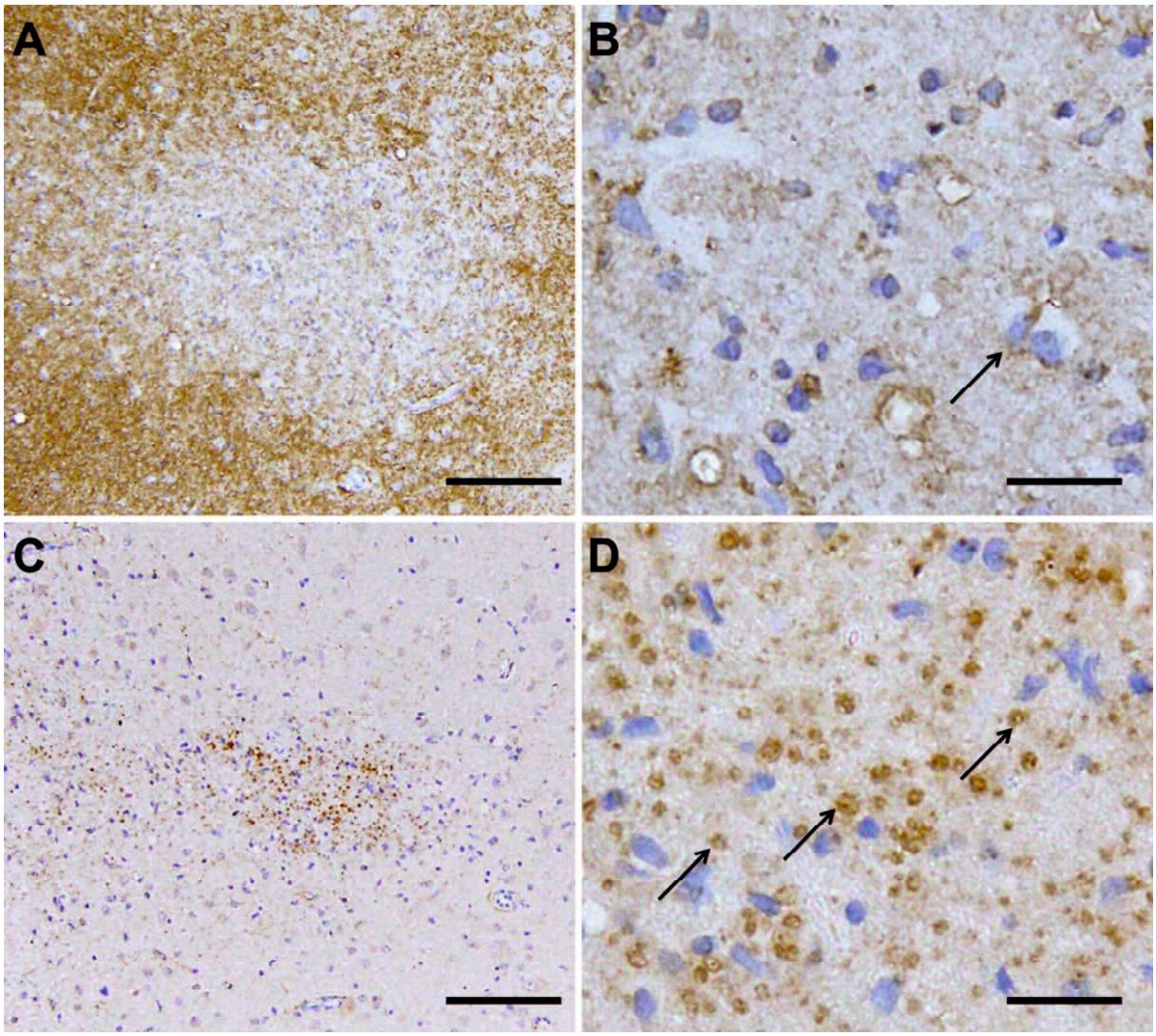

Figure 3. Immunohistochemical expression of glutamate transporter 1 (GLT-1) and glutamate in the nucleus reuniens of rat having status epilepticus. GLT-1 immunoreactivity is focally decreased (A). There is a small number of GLT-1-positive astrocytes (B, arrow). Strong glutamate immunoreactivity is observed and confined to the lesion (C). The glutamate immunoreactivity is observed in the neuropil (D, arrows). Immunohistochemistry for GLT-1 (A, B) and for glutamate (C, D). Bars, 100 μm (A, C) and 20 μm (B, D).

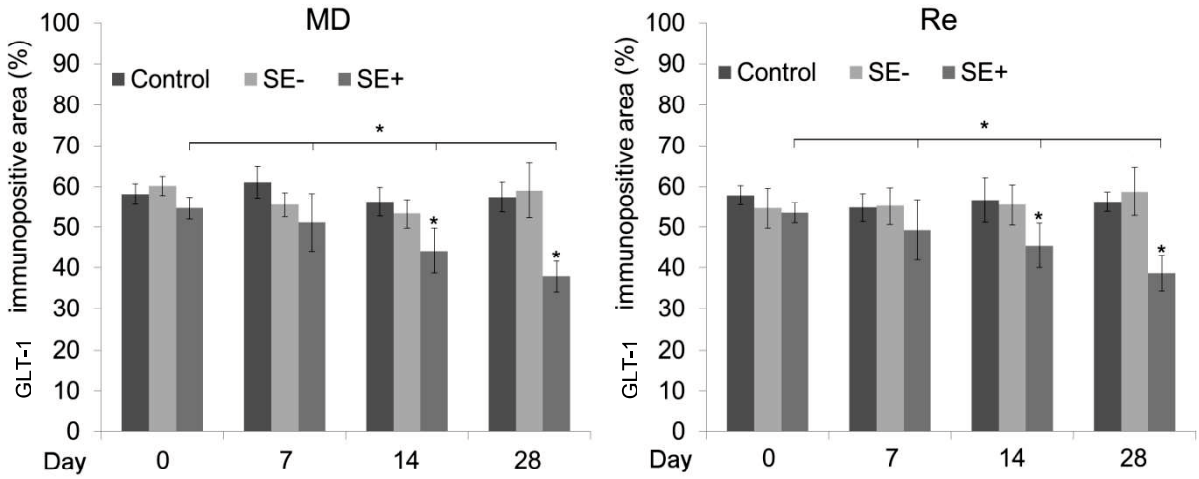

Figure 4. The percentage of glutamate transpoter 1 (GLT-1) immunopositive area in the mediodorsal nucleus (MD) and nucleus reuniens (Re). The data represent mean values ± standard deviation. *P < 0.05. Abbrev. SE -, rats without status epilepticus; SE +, rats having status epilepticus.

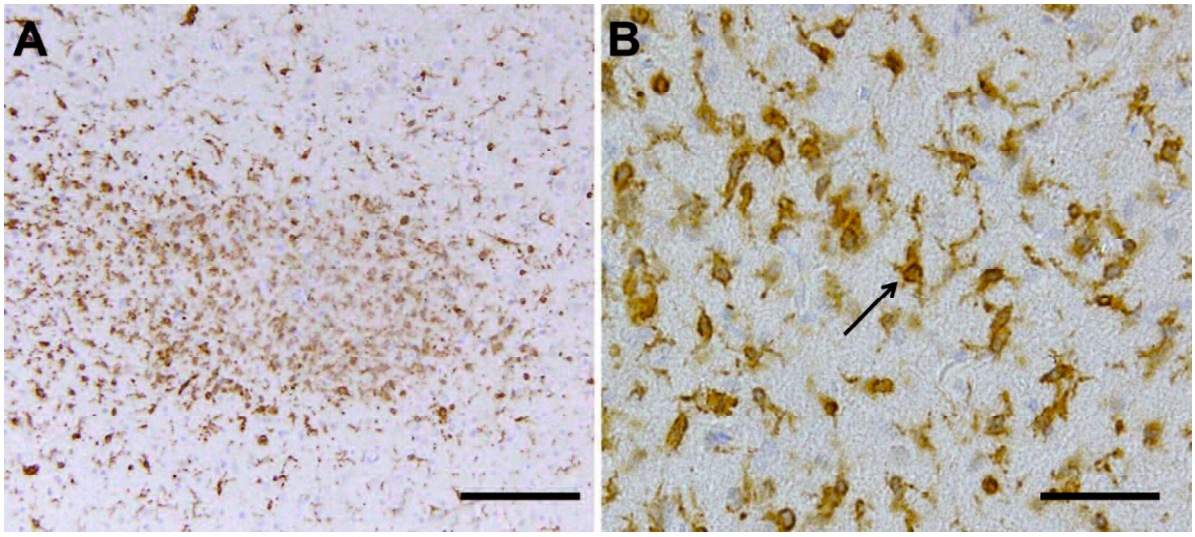

Figure 5. Microglial proliferation in the nucleus reuniens of rat having status epilepticus. Note focal accumulation of Iba-1-positive microglial cells within the lesion (A), mostly showing an activated shape (swollen cell bodies and long processes) (B, arrow). Immunohistochemistry for Iba-1. Bars, 100 μm (A), 20 μm (B).

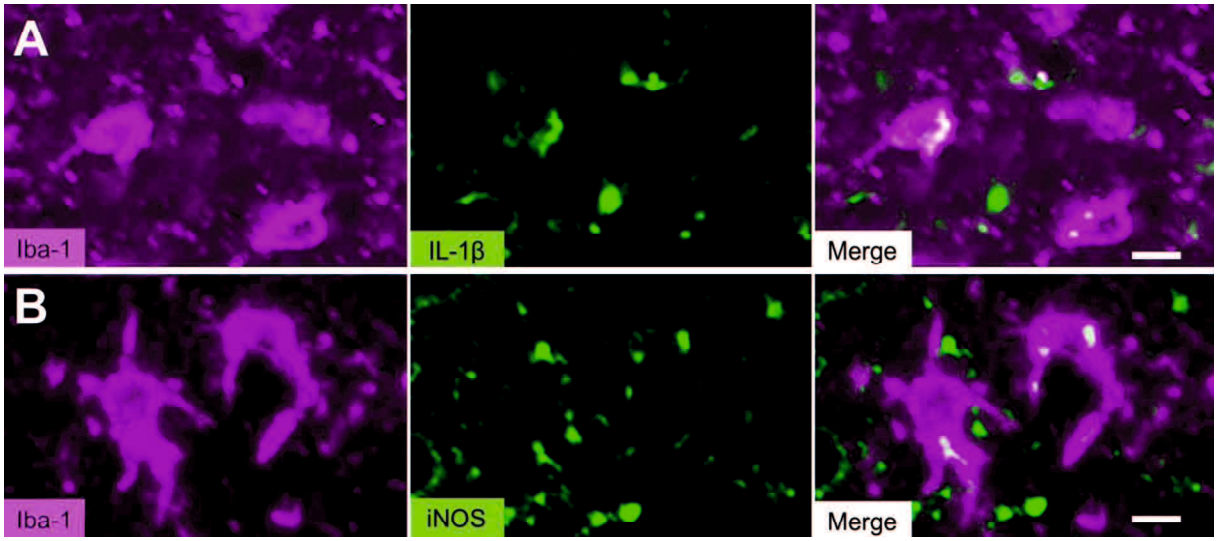

Figure 6. Expressions of interleukin-1 beta (IL-1β) and inducible nitric oxide synthase (iNOS) in microglial cells in the midline thalamic regions. Double immunofluorescence for Iba-1 (magenta), and IL-1β (A) or iNOS (B) (green). Bars, 10 μm.

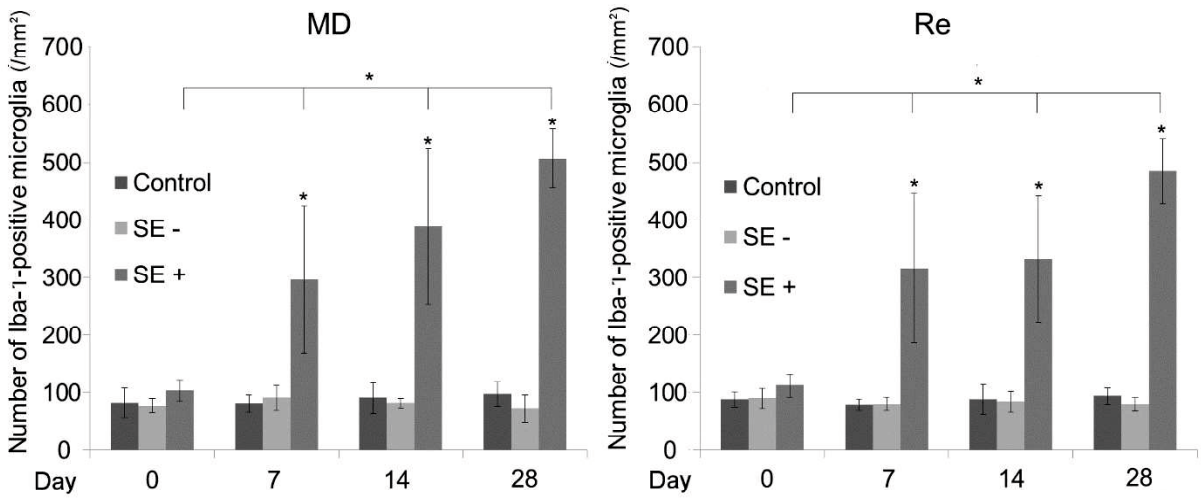

Figure 7. The number of Iba-1-positive microglia in the mediodorsal nucleus (MD) and nucleus reuniens (Re). The data represent mean values ± standard deviation. *P < 0.05. Abbrev. SE -, rats without status epilepticus; SE +, rats having status epilepticus.

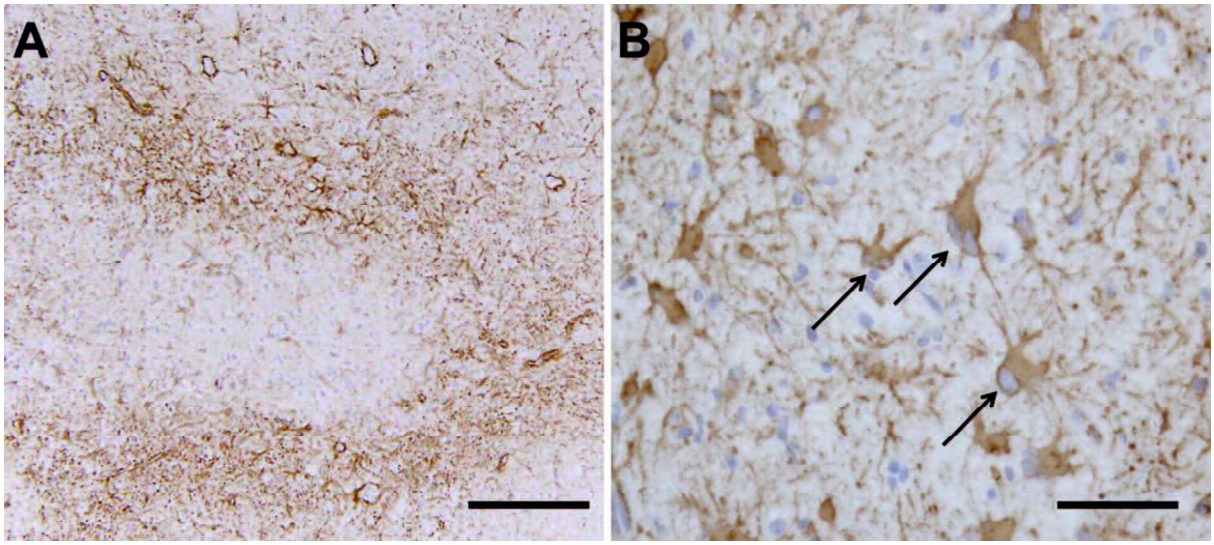

Figure 8. Reactive astrocytes in the nucleus reuniens of rat having status epilepticus. Glial fibrillary acidic protein (GFAP) immunoreactivity is detected in reactive astrocytes in the lesion, whereas proliferation of GFAP-positive astrocytes are observed in the peri-lesional area (A). Note GFAP-positive reactive astrocytes showing swollen cytoplasm, thick short processes and occasional multiple nuclei (B, arrows) within the lesion. Immunohistochemistry for GFAP (A, B). Bars, 100 μm (A), 20 μm (B).

Tables

Table 1. Summary of the histological and immunohistochemical findings in the mediodorsal nucleus (MD) and reuniens nucleus (Re) of rats having status epilepticus.

	Day	n	Neuronal death†	Calcification	Glutamate	Microglia‡	Reactive astrocyte§	GLT-1¶
MD	0	5	-	-	-	+	-	+++
	2	2	-	-	-	++	-	+++
	7	2	-	-	-	++	+	++
		5	+	+	+	++ to +++	++	+ to ++
	14	3	-	-	-	++	++	++
		5	+	+	+	+++	++	+
	28	5	+	+	+	+++	++	+
Re	0	5	-	-	-	+	-	+++
	2	2	-	-	-	++	-	+++
	7	2	-	-	-	++	+	++
		5	+	+	+	++ to +++	++	+ to ++
	14	3	-	-	-	++	+ to ++	++
		5	+	+	+	+++	++	+
	28	5	+	+	+	+++	++	+

†In the column for 'neuronal death', '+' indicates the presence of both neurons with ischemic-like changes and Fluoro-Jade C staining-positive cells. ‡The column for 'microglia' represents the number of Iba-1-positive microglia per 1 mm^2; '+' indicates less than 200, '++' indicates 200 or more but less than 400, and '+++' indicates 400 or more. §The column for 'reactive astrocyte" represents the number of GFAP-positive astrocytes showing swollen cytoplasm, thick short processes, and occasional multiple nuclei in the lesion, '+' indicates less than 15, and '++' indicates 15 or more when observed with x40 objective lens. ¶The coloum for GLT-1 represents the percentage of

glutamate transporter 1-immunoreactive area calculated by means of computer-assisted image analysis using the digital images taken with x10 objective lens (1.3 mm^2); '+++' indicates 50% or more, '++' indicates less than 50% but more than 45%, '+' indicates 45% or less.

GENERAL DISCUSSION AND CONCLUSION

In the first chapter, the relationship of angiogenesis and microglial activation to seizure-induced neuronal death associated with GLT-1 downregulation in the cerebrum of familial epileptic Shetland Sheepdogs was demonstrated (Figure 1). Consistent distribution of angiogenesis and microglial activation indicates the relationship to seizure-induced neuronal death. Microglial activation may have a major role in the GLT-1 downregualtion. Further, VEGF-expression associated with angiogenesis might enhance and spread the microglial activation.

TNF-α, which was expressed in the activated microglia in the cerebrum of Shetland Sheepdogs, is thought to be responsible for GLT-1 downregration. Microglia are resident immune cells in the central nervous system (Graeber et al., 2010). Activated microglia express pro-inflammatory cytokines, as well as in this study (Graeber et al., 2010). TNF-α, a pro-inflammatory cytokine expressed in the activated microglia of familial Shetland Sheepdogs, has been reported to induce GLT-1 downregulation that results in neuronal death (Carmen et al., 2009).

VEGF-expression is thought to enhance and spread the microglial activation in and around the lesions of familial Shetland Sheepdogs. VEGF is sometimes called as a

double edged-sword in the brain after seizures, because the role of VEGF is either protective (e.g. angiogenesis) or destructive (e.g. neuroinflammation) (Croll et al., 2004). In this study, VEGF-expression in neurons and glial cells (astrocytes and microglia) is firstly considered to induce angiogenesis for protection of neurons, however, VEGFR-1-expression in the activated microglia suggests an induction of microglial activation by VEGF. VEGF has been reported to activate microglia via VEGFR-1 and induce an inflammatory response which includes expression of TNF-α and IL-6 (Croll et al., 2004; Forstreuter et al., 2002; Yoo et al., 2005). In the cerebrum of the familial Shetland Sheepdogs, VEGF expressed in neurons and glial cells could activate microglia and induce overexpression of pro-inflammatory cytokines. In addition, the distribution of VEGF-positive cells and activated microglia around the lesions where neuronal death was not observed suggests that VEGF has a role in the expansion of the lesion via microglial activation.

In the second chapter, the progress of the lesion of seizure-induced neuronal death in the thalamus of kainic acid-treated rat was demonstrated. GLT-1 downregulation and microglial activation are considered as a cause of seizure-induced neuronal death (Figure 2). From day 7 after induction of seizures, the seizure-induced neuronal death was found in the midline thalamic regions. These thalamic regions were always

associated with the GLT-1 downregulation and microglial activation. Further, some animals at day 7 showed mild GLT-1 downregulation and microglial activation in the midline thalamic regions without neuronal death.

GLT-1 downregulation can cause neuronal death due to glutamate excitotoxicity (Anderson et al., 2000; Rodríguez et al., 2000). Immunohistochemically, accumulation of glutamate is suggested in the lesions of neuronal death. It has been reported that neuronal death caused by glutamate excitotoxicity is frequently associated with calcification (calcium deposition), as well as in this study (Gayoso et al., 2003; Rodríguez et al., 2000).

Pro-inflammatory cytokines and nitric oxide induced by the activated microglia in the lesion might be responsible for the GLT-1 downregulation. Both IL-1β and nitric oxide has been reported to induce GLT-1 downregulation (Yamada et al., 2006; Prow et al., 2008). Though the pathogenesis is not known in detail, seizures have been reported to activate microglia (Avignone et al., 2008).

In summary, glutamate toxicity due to GLT-1 downregulation is considered to be a cause of seizure-induced neuronal death in the cerebrum of both familial epileptic Shetland Sheepdogs and the thalamus of kainic acid-treated rats. In addition,

neuroinflammation, particularly microgrial activation, may induce GLT-1 downregulation in the brain after epileptic seizures.

In conclusion, this study demonstrated that seizure can induce various pathological changes including both neuroprotective (angiogenesis) and neurodestructive (microglial activation and GLT-1 downregulation). These changes were considered to a cause of seizure-induced neuronal death resulting in the sequellae of brain dysfunctions (Figure 3). However, the current studies did not investigate other possible mechanisms of seizure-induced neuronal death (e.g. hypoperfusion, blood-brain barrier breakdown, neuroinflammation). Further study on prolonged period after seizure, other animals and animal models of epilepsy are needed. Seizure-induced neuronal death is considered to be caused as a result of various pathologic changes after seizures. Further study is required for the individual pathologic changes.

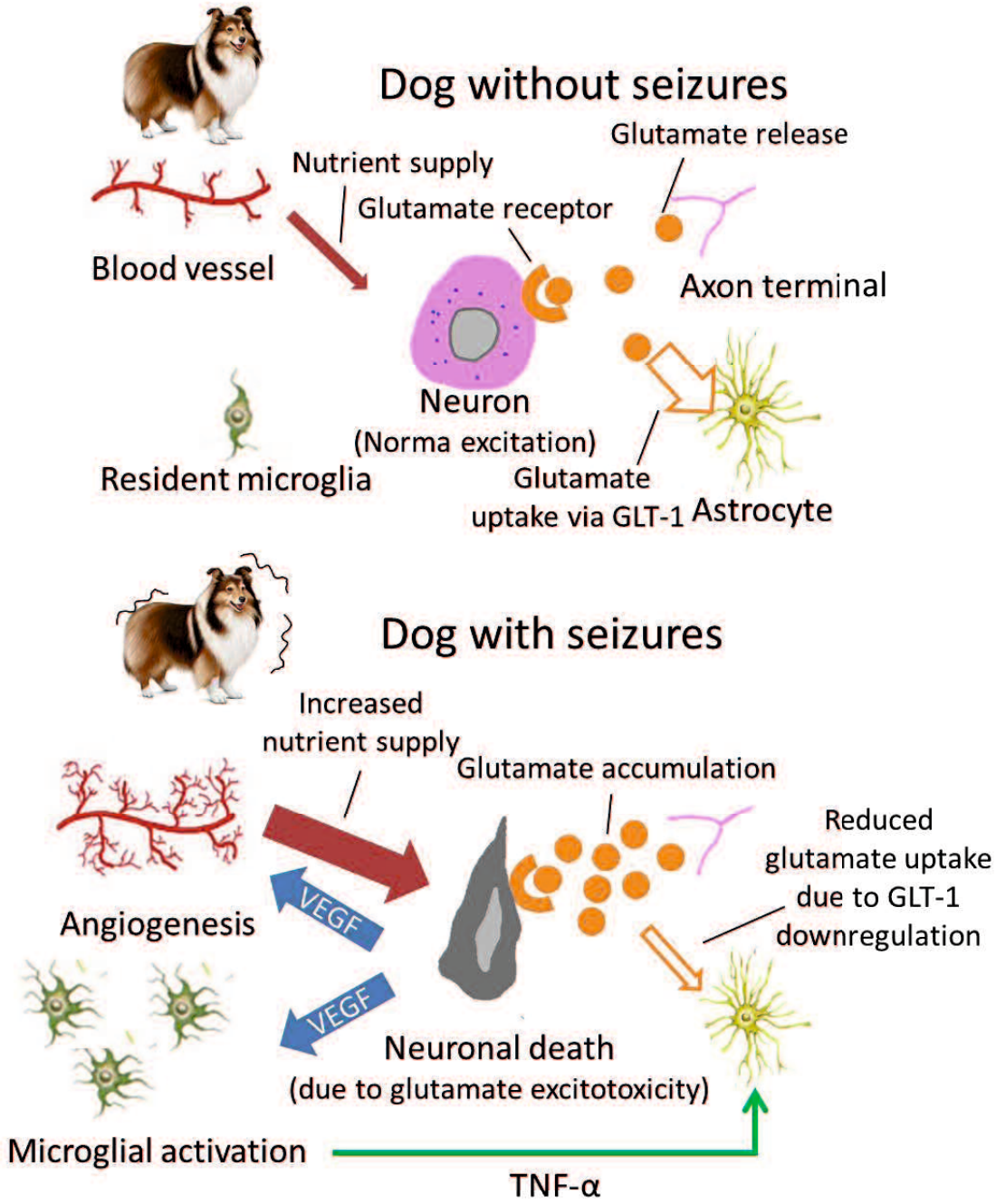

Figure 1. Schematic diagram shows the normal relationship among neuron, glial cells and blood vessels in the cerebrum of familial Shetland Sheepdogs without seizures (above) and the possible mechanism of seizure-induced neuronal death in the familial Shetland Sheepdogs with seizures (below).

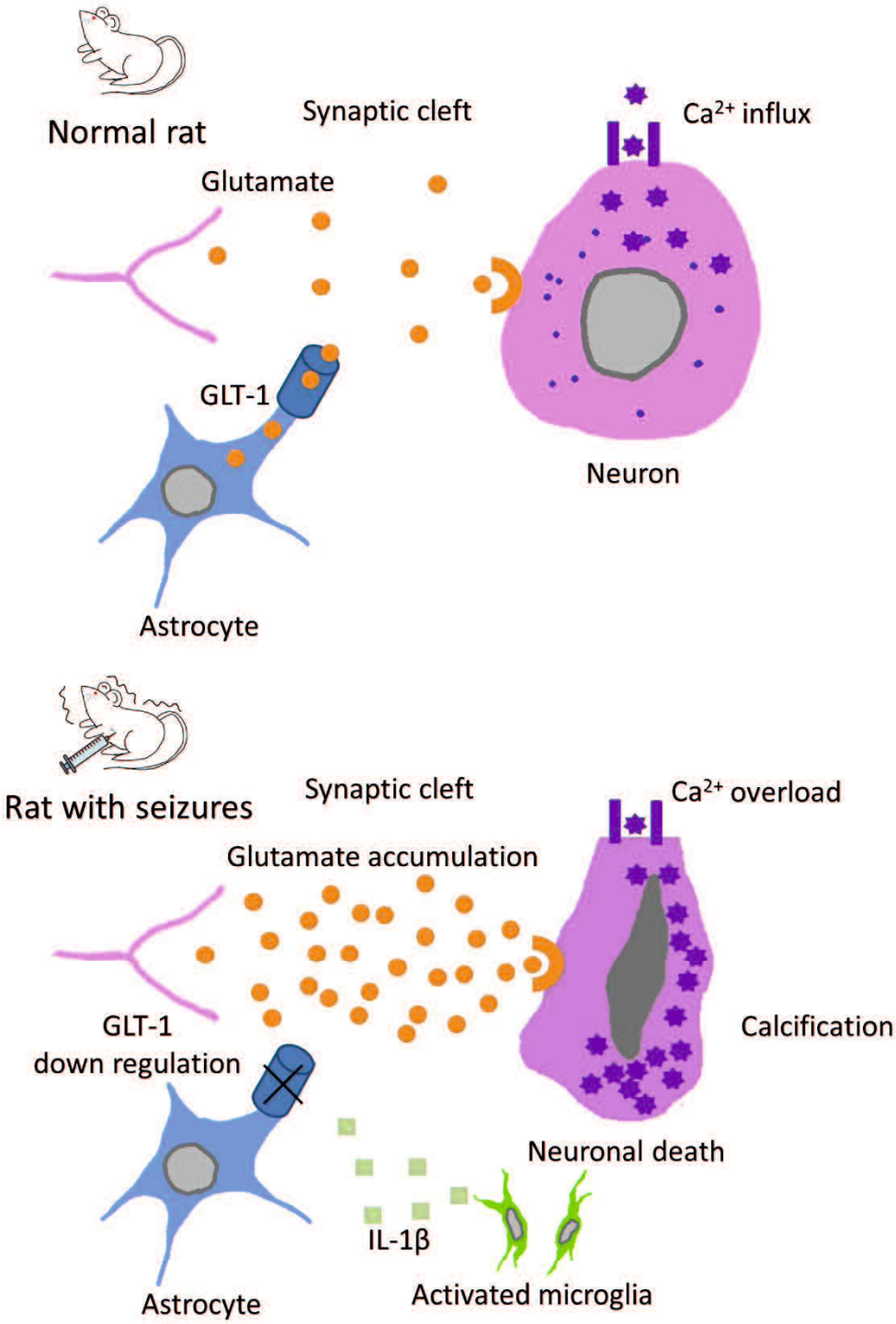

Figure 2. Schematic diagram shows the normal synaptic cleft of the rat without seizures (above) and the possible mechasim of seizure-induced neuronal death in the cerebrum of rat with seizures (below).

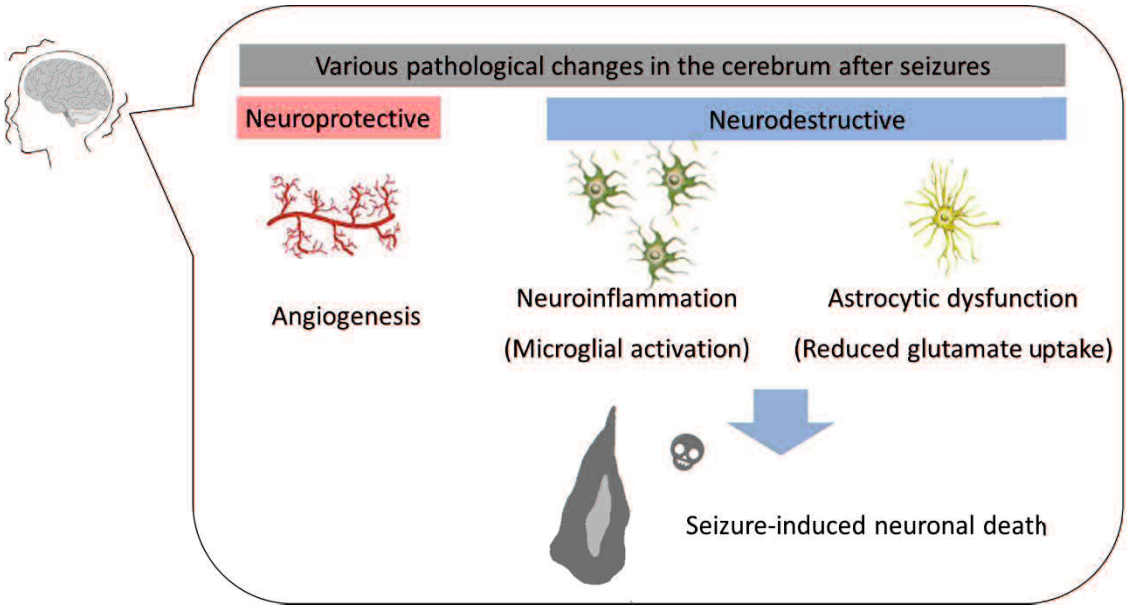

Figure 3. Schematic diagram shows the possible risk of epileptic seizures. Epileptic seizures can induce several pathological changes, which have neuroprotective or neurodestructive effects, in the cerebrum. The neurodestrcutive effects sometimes result in seizure-induced neuronal death.

ACKNOWLEDGMENTS

The research for this Ph.D. The thesis was carried out at Department of Veterinary Pathology, Faculty of Agriculture, Tottori University. I am deeply grateful to my supervisor Professor Dr. Takehito Morita (Department of Veterinary Pathology, Tottori University) for his guidance and his dedication and encouragement during this work. I also thank Professor Dr. Akinori Shimada (Laboratory of Pathology, School of Life and Environmental Science, Azabu University) for his expert advice and encouragement during the whole course of this thesis work. I also want to thank all the other co-authors for their contributions in this work.

I warmly thank my collaborators in the epilepsy team, Ms. Haruna Kurokawa and Ms. Hiroko Suzuki for their fruitful collaboration. I would like to thank Ms. Misaki Naota (Pharmaceuticals and Medical Devices Agency, Japan), and Mr. Kasem Rattanapinyopituk (National Cancer Institute of Thailand) for giving excellent advice in the study. I am grateful to the whole students of Department of Veterinary Pathology, Tottori University for their continuous support and assistance. Finally, I am especially grateful to my family for the encouragement given to me, and for supporting me in all my efforts by over the years.

REFERENCES

Abbott, N. J., Patabendige, A. A., Dolman, D. E., Yusof, S. R. and Begley, D. J. (2010). Structure and function of the blood-brain barrier. *Neurobiol Dis,* **37,** 13-25.

Alessio, A., Bonilha, L., Rorden, C., Kobayashi, E., Min, L. L., Damasceno, B. P. and Cendes, F. (2006). Memory and language impairments and their relationships to hippocampal and perirhinal cortex damage in patients with medial temporal lobe epilepsy. *Epilepsy Behav,* **8,** 593-600.

Allan, S. M. and Rothwell, N. J. (2001). Cytokines and acute neurodegeneration. *Nat Rev Neurosci,* **2,** 734-744.

Anderson, C. M. and Swanson, R. A. (2000). Astrocyte glutamate transport: review of properties, regulation, and physiological functions. *Glia,* **32,** 1-14.

Avignone, E., Ulmann, L., Levavasseur, F., Rassendren, F. and Audinat, E. (2008). Status epilepticus induces a particular microglial activation state characterized by enhanced purinergic signaling. *J Neurosci,* **28,** 9133-9144.

Balkhi H. J., Gul T., Banday M. Z. and Haq E. (2014). Glutamate excitotoxicity: an insight into the mechanism. *Int J Adv Res* **2**, 361-373.

Bertram, E. H. (2012). Neuronal circuits in epilepsy: Do they matter? *Exp Neurol*.

Blume, W. T., Luders, H. O., Mizrahi, E., Tassinari, C., van Emde Boas, W. and Engel, J., Jr. (2001). Glossary of descriptive terminology for ictal semiology: report of the ILAE task. *Epilepsia,* **42,** 1212-1218.

Brown, G. C. and Neher, J. J. (2010). Inflammatory neurodegeneration and mechanisms of microglial killing of neurons. *Mol Neurobiol,* **41,** 242-247.

Buckmaster, P. S. (2004). Laboratory animal models of temporal lobe epilepsy. *Comp Med,* **54,** 473-485.

Buckmaster, P. S., Smith, M. O., Buckmaster, C. L., LeCouteur, R. A. and Dudek, F. E. (2002). Absence of temporal lobe epilepsy pathology in dogs with medically intractable epilepsy. *J Vet Intern Med,* **16,** 95-99.

Campbell, I. L., Abraham, C. R., Masliah, E., Kemper, P., Inglis, J. D., Oldstone, M. B. and Mucke, L. (1993). Neurologic disease induced in transgenic mice by cerebral overexpression of interleukin 6. *Proc Natl Acad Sci U S A,* **90,** 10061-10065.

Carmen, J., Rothstein, J. D. and Kerr, D. A. (2009). Tumor necrosis factor-alpha modulates glutamate transport in the CNS and is a critical determinant of outcome from viral encephalomyelitis. *Brain Res,* **1263,** 143-154.

Choi, D. W. (1988). Glutamate neurotoxicity and diseases of the nervous system. In: *Neuron*, Vol. 1, United States, pp. 623-634.

Choy, M., Wells, J. A., Thomas, D. L., Gadian, D. G., Scott, R. C. and Lythgoe, M. F. (2010). Cerebral blood flow changes during pilocarpine-induced status epilepticus activity in the rat hippocampus. *Exp Neurol,* **225,** 196-201.

Ciumas, C., Lindstrom, P., Aoun, B. and Savic, I. (2008). Imaging of odor perception delineates functional disintegration of the limbic circuits in mesial temporal lobe epilepsy. *Neuroimage,* **39,** 578-592.

Crespel, A., Coubes, P., Rousset, M. C., Brana, C., Rougier, A., Rondouin, G., Bockaert, J., Baldy-Moulinier, M. and Lerner-Natoli, M. (2002). Inflammatory reactions in human medial temporal lobe epilepsy with hippocampal sclerosis. *Brain Res,* **952,** 159-169.

Croll, S. D., Goodman, J. H. and Scharfman, H. E. (2004). Vascular endothelial growth factor (VEGF) in seizures: a double-edged sword. *Adv Exp Med Biol,* **548,** 57-68.

Curia, G., Longo, D., Biagini, G., Jones, R. S. and Avoli, M. (2008). The pilocarpine model of temporal lobe epilepsy. *J Neurosci Methods,* **172,** 143-157.

Dahl, L. K. A simple and sensitive histochemical method for calcium, 1952, pp. 474-479.

Duncan, J. S. (2002). Seizure-induced neuronal injury: human data. *Neurology,* **59,** S15-20.

Dupont, P., Zaknun, J. J., Maes, A., Tepmongkol, S., Vasquez, S., Bal, C. S., Van Paesschen, W., Carpintiero, S., Locharernkul, C. and Dondi, M. (2009). Dynamic perfusion patterns in temporal lobe epilepsy. *Eur J Nucl Med Mol Imaging,* **36,** 823-830.

Dutuit, M., Touret, M., Szymocha, R., Nehlig, A., Belin, M. F. and Didier-Bazes, M. (2002). Decreased expression of glutamate transporters in genetic absence epilepsy rats before seizure occurrence. *J Neurochem,* **80,** 1029-1038.

Forstreuter, F., Lucius, R. and Mentlein, R. (2002). Vascular endothelial growth factor induces chemotaxis and proliferation of microglial cells. *J Neuroimmunol,* **132,** 93-98.

Fujikawa, D. G., Itabashi, H. H., Wu, A. and Shinmei, S. S. (2000). Status epilepticus-induced neuronal loss in humans without systemic complications or epilepsy. *Epilepsia,* **41,** 981-991.

Färber, K. and Kettenmann, H. (2006). Purinergic signaling and microglia. *Pflugers Arch,* **452,** 615-621.

Gadient, R. A. and Otten, U. H. (1997). Interleukin-6 (IL-6)--a molecule with both beneficial and destructive potentials. *Prog Neurobiol,* **52,** 379-390.

Gayoso, M. J., Al-Majdalawi, A., Garrosa, M., Calvo, B. and Díaz-Flores, L. (2003). Selective calcification of rat brain lesions caused by systemic administration of kainic acid. *Histol Histopathol,* **18,** 855-869.

Goldberg, E. M. and Coulter, D. A. (2013). Mechanisms of epileptogenesis: a convergence on neural circuit dysfunction. *Nat Rev Neurosci,* **14,** 337-349.

Gorter, J. A., Gonçalves Pereira, P. M., van Vliet, E. A., Aronica, E., Lopes da Silva, F. H. and Lucassen, P. J. (2003). Neuronal cell death in a rat model for mesial temporal lobe epilepsy is induced by the initial status epilepticus and not by later repeated spontaneous seizures. *Epilepsia,* **44,** 647-658.

Graeber, M. B. and Streit, W. J. (2010). Microglia: biology and pathology. *Acta Neuropathol,* **119,** 89-105.

Helms, G., Ciumas, C., Kyaga, S. and Savic, I. (2006). Increased thalamus levels of glutamate and glutamine (Glx) in patients with. *J Neurol Neurosurg Psychiatry,* **77,** 489-494.

Heneka, M. T., O'Banion, M. K., Terwel, D. and Kummer, M. P. (2010). Neuroinflammatory processes in Alzheimer's disease. *J Neural Transm,* **117,** 919-947.

Herberg, L. J., Grottick, A. and Rose, I. C. (1995). Nitric oxide synthesis, epileptic seizures and kindling. *Psychopharmacology (Berl),* **119,** 115-123.

Herman, S. T., Takeoka, M., Hughes, J. R. and Drislane, F. W. (2011). Electroencephalography in clinical epilepsy research. *Epilepsy Behav,* **22,** 126-133.

Holmes, G. L. (2002). Seizure-induced neuronal injury: animal data. *Neurology,* **59,** S3-6.

Ingvar, M., Morgan, P. F. and Auer, R. N. (1988). The nature and timing of excitotoxic neuronal necrosis in the cerebral cortex, hippocampus and thalamus due to flurothyl-induced status epilepticus. *Acta Neuropathol,* **75,** 362-369.

Jacek, S., Stevenson, R. J. and Miller, L. A. (2007). Olfactory dysfunction in temporal lobe epilepsy: a case of ictus-related parosmia. *Epilepsy Behav,* **11,** 466-470.

Kanner, A. M. (2011). Depression and epilepsy: A bidirectional relation? *Epilepsia,* **52 Suppl 1,** 21-27.

Kiaei, M., Petri, S., Kipiani, K., Gardian, G., Choi, D. K., Chen, J., Calingasan, N. Y., Schafer, P., Muller, G. W., Stewart, C., Hensley, K. and Beal, M. F. (2006). Thalidomide and lenalidomide extend survival in a transgenic mouse model of amyotrophic lateral sclerosis. *J Neurosci,* **26,** 2467-2473.

Kim, S. U. and de Vellis, J. (2005). Microglia in health and disease. *J Neurosci Res,* **81,** 302-313.

Kuwabara, T., Hasegawa, D., Ogawa, F., Kobayashi, M., Fujita, M., Suzuki, H., Matsuki, N. and Orima, H. (2010). A familial spontaneous epileptic feline strain: a novel model of idiopathic/genetic epilepsy. *Epilepsy Res,* **92,** 85-88.

Kwan, P. and Brodie, M. J. (2000). Early identification of refractory epilepsy. *N Engl J Med,* **342,** 314-319.

Lau, A. and Tymianski, M. (2010). Glutamate receptors, neurotoxicity and neurodegeneration. *Pflugers Arch,* **460,** 525-542.

Lee, C. L., Hannay, J., Hrachovy, R., Rashid, S., Antalffy, B. and Swann, J. W. (2001). Spatial learning deficits without hippocampal neuronal loss in a model of early-onset epilepsy. *Neuroscience,* **107,** 71-84.

Levesque, M. and Avoli, M. (2013). The kainic acid model of temporal lobe epilepsy. *Neurosci Biobehav Rev,* **37,** 2887-2899.

McKenna, J. T. and Vertes, R. P. (2004). Afferent projections to nucleus reuniens of the thalamus. *J Comp Neurol,* **480,** 115-142.

Meldrum, B. S. (1993). Excitotoxicity and selective neuronal loss in epilepsy. *Brain Pathol,* **3,** 405-412.

Morimoto, K., Fahnestock, M. and Racine, R. J. (2004). Kindling and status epilepticus models of epilepsy: rewiring the brain. *Prog Neurobiol,* **73,** 1-60.

Morita, T., Shimada, A., Takeuchi, T., Hikasa, Y., Sawada, M., Ohiwa, S., Takahashi, M., Kubo, N., Shibahara, T., Miyata, H. and Ohama, E. (2002). Cliniconeuropathologic findings of familial frontal lobe epilepsy in Shetland sheepdogs. *Can J Vet Res,* **66,** 35-41.

Morita, T., Takahashi, M., Takeuchi, T., Hikasa, Y., Ikeda, S., Sawada, M., Sato, K., Shibahara, T. and Shimada, A. (2005). Changes in extracellular neurotransmitters in the cerebrum of familial idiopathic epileptic shetland sheepdogs using an intracerebral microdialysis technique and immunohistochemical study for glutamate metabolism. *J Vet Med Sci,* **67,** 1119-1126.

Nairismägi, J., Gröhn, O. H., Kettunen, M. I., Nissinen, J., Kauppinen, R. A. and Pitkänen, A. (2004). Progression of brain damage after status epilepticus and its association with epileptogenesis: a quantitative MRI study in a rat model of temporal lobe epilepsy. *Epilepsia,* **45,** 1024-1034.

Najjar, S., Pearlman, D., Miller, D. C. and Devinsky, O. (2011). Refractory epilepsy associated with microglial activation. *Neurologist,* **17,** 249-254.

Nakamura, K., Wright, D., Kondoh, Y., Mizusawa, S. and Kinoshita, T. (2008). Quantitative accuracy of delayed hyperperfusion in MRI of transient ischemia in. *Conf Proc IEEE Eng Med Biol Soc,* **2008,** 839-842.

Natsume, J., Bernasconi, N., Andermann, F. and Bernasconi, A. (2003). MRI volumetry of the thalamus in temporal, extratemporal, and idiopathic generalized epilepsy. *Neurology,* **60,** 1296-1300.

Ndode-Ekane, X. E., Hayward, N., Gröhn, O. and Pitkänen, A. (2010). Vascular changes in epilepsy: functional consequences and association with network plasticity in pilocarpine-induced experimental epilepsy. *Neuroscience,* **166,** 312-332.

Oby, E. and Janigro, D. (2006). The blood-brain barrier and epilepsy. *Epilepsia,* **47,** 1761-1774.

Paxinos G and Watson C. The Rat Brain in Stereotaxic Coordinates, 2nd edn. San Diego: Academic Press Inc., 1986.

Pinheiro, P. and Mulle, C. (2006). Kainate receptors. *Cell Tissue Res,* **326,** 457-482.

Proper, E. A., Hoogland, G., Kappen, S. M., Jansen, G. H., Rensen, M. G., Schrama, L. H., van Veelen, C. W., van Rijen, P. C., van Nieuwenhuizen, O., Gispen, W. H. and de Graan, P. N. (2002). Distribution of glutamate transporters in the hippocampus of patients with. *Brain,* **125,** 32-43.

Prow, N. A. and Irani, D. N. (2008). The inflammatory cytokine, interleukin-1 beta, mediates loss of astroglial glutamate transport and drives excitotoxic motor neuron injury in the spinal cord during acute viral encephalomyelitis. *J Neurochem,* **105,** 1276-1286.

Rajdev, S. and Reynolds, I. J. (1994). Glutamate-induced intracellular calcium changes and neurotoxicity in cortical neurons in vitro: effect of chemical ischemia. *Neuroscience,* **62,** 667-679.

Rao, V. L., Dogan, A., Todd, K. G., Bowen, K. K., Kim, B. T., Rothstein, J. D. and Dempsey, R. J. (2001). Antisense knockdown of the glial glutamate transporter GLT-1, but not the. *J Neurosci,* **21,** 1876-1883.

Rigau, V., Morin, M., Rousset, M. C., de Bock, F., Lebrun, A., Coubes, P., Picot, M. C., Baldy-Moulinier, M., Bockaert, J., Crespel, A. and Lerner-Natoli, M. (2007). Angiogenesis is associated with blood-brain barrier permeability in temporal lobe epilepsy. *Brain,* **130,** 1942-1956.

Rijkers, K., Majoie, H. J., Hoogland, G., Kenis, G., De Baets, M. and Vles, J. S. (2009). The role of interleukin-1 in seizures and epilepsy: a critical review. *Exp Neurol,* **216,** 258-271.

Rizzi, M., Perego, C., Aliprandi, M., Richichi, C., Ravizza, T., Colella, D., Veliskova, J., Moshe, S. L., De Simoni, M. G. and Vezzani, A. (2003). Glia activation and cytokine increase in rat hippocampus by kainic acid-induced status epilepticus during postnatal development. *Neurobiol Dis,* **14,** 494-503.

Rodríguez, M. J., Bernal, F., Andrés, N., Malpesa, Y. and Mahy, N. (2000). Excitatory amino acids and neurodegeneration: a hypothetical role of calcium precipitation. *Int J Dev Neurosci,* **18,** 299-307.

Rothstein, J. D., Martin, L., Levey, A. I., Dykes-Hoberg, M., Jin, L., Wu, D., Nash, N. and Kuncl, R. W. (1994). Localization of neuronal and glial glutamate transporters. *Neuron,* **13,** 713-725.

Ryu, J. K., Cho, T., Choi, H. B., Wang, Y. T. and McLarnon, J. G. (2009). Microglial VEGF receptor response is an integral chemotactic component in Alzheimer's disease pathology. *J Neurosci,* **29,** 3-13.

Salami, P., Levesque, M., Benini, R., Behr, C., Gotman, J. and Avoli, M. (2014). Dynamics of interictal spikes and high-frequency oscillations during epileptogenesis in temporal lobe epilepsy. *Neurobiol Dis,* **67,** 97-106.

Sallmann, S., Jüttler, E., Prinz, S., Petersen, N., Knopf, U., Weiser, T. and Schwaninger, M. (2000). Induction of interleukin-6 by depolarization of neurons. *J Neurosci,* **20,** 8637-8642.

Samuelsson, C., Kumlien, E., Flink, R., Lindholm, D. and Ronne-Engstrom, E. (2000). Decreased cortical levels of astrocytic glutamate transport protein GLT-1 in a rat model of posttraumatic epilepsy. *Neurosci Lett,* **289,** 185-188.

Sander, J. W. (2003). The epidemiology of epilepsy revisited. *Curr Opin Neurol,* **16,** 165-170.

Sarkisova, K. Y., Midzianovskaia I. S. and Kulikov, M. A. (2003). Depressive-like behavioral alterations and c-fos expression in the dopaminergic brain regions in WAG/Rij rats with genetic absence epilepsy. *Behav Brain Res*, **144,** 211-216.

Schipke, C. G., Boucsein, C., Ohlemeyer, C., Kirchhoff, F. and Kettenmann, H. (2002). Astrocyte Ca2+ waves trigger responses in microglial cells in brain slices. *Faseb j,* **16,** 255-257.

Seifert, G., Carmignoto, G. and Steinhauser, C. (2010). Astrocyte dysfunction in epilepsy. In: *Brain Res Rev*, Vol. 63, 2009 Elsevier B.V, Netherlands, pp. 212-221.

Shapiro, L. A., Wang, L. and Ribak, C. E. (2008). Rapid astrocyte and microglial activation following pilocarpine-induced seizures. *Epilepsia,* **49 Suppl 2,** 33-41.

Somera-Molina, K. C., Nair, S., Van Eldik, L. J., Watterson, D. M. and Wainwright, M. S. (2009). Enhanced microglial activation and proinflammatory cytokine upregulation are linked to increased susceptibility to seizures and neurologic injury in a 'two-hit' seizure model. *Brain Res,* **1282,** 162-172.

Sonnewald, U., Westergaard, N. and Schousboe, A. (1997). Glutamate transport and metabolism in astrocytes. *Glia,* **21,** 56-63.

Sutula, T. P., Cavazos, J. E. and Woodard, A. R. (1994). Long-term structural and functional alterations induced in the hippocampus by kindling: implications for memory dysfunction and the development of epilepsy. *Hippocampus,* **4,** 254-258.

Takeuchi, H., Jin, S., Wang, J., Zhang, G., Kawanokuchi, J., Kuno, R., Sonobe, Y., Mizuno, T. and Suzumura, A. (2006). Tumor necrosis factor-alpha induces neurotoxicity via glutamate release from hemichannels of activated microglia in an autocrine manner. *J Biol Chem,* **281,** 21362-21368.

Tham, W. W., Stevenson, R. J. and Miller, L. A. (2009). The functional role of the medio dorsal thalamic nucleus in olfaction. *Brain Res Rev,* **62,** 109-126.

Thomas, W. B. (2010). Idiopathic epilepsy in dogs and cats. *Vet Clin North Am Small Anim Pract,* **40,** 161-179.

Ueda, Y., Doi, T., Tokumaru, J., Yokoyama, H., Nakajima, A., Mitsuyama, Y., Ohya-Nishiguchi, H., Kamada, H. and Willmore, L. J. (2001). Collapse of extracellular glutamate regulation during epileptogenesis: down-regulation and functional failure of glutamate transporter function in rats with chronic seizures induced by kainic acid. *J Neurochem,* **76,** 892-900.

van Vliet, E. A., da Costa Araújo, S., Redeker, S., van Schaik, R., Aronica, E. and Gorter, J. A. (2007). Blood-brain barrier leakage may lead to progression of temporal lobe epilepsy. *Brain,* **130,** 521-534.

Vertes, R. P. (2002). Analysis of projections from the medial prefrontal cortex to the thalamus in the rat, with emphasis on nucleus reuniens. *J Comp Neurol,* **442,** 163-187.

Vezzani, A., Balosso, S. and Ravizza, T. (2008a). The role of cytokines in the pathophysiology of epilepsy. *Brain Behav Immun,* **22,** 797-803.

Vezzani, A., Ravizza, T., Balosso, S. and Aronica, E. (2008b). Glia as a source of cytokines: implications for neuronal excitability and survival. *Epilepsia,* **49 Suppl 2,** 24-32.

Walton, M., Connor, B., Lawlor, P., Young, D., Sirimanne, E., Gluckman, P., Cole, G. and Dragunow, M. (1999). Neuronal death and survival in two models of hypoxic-ischemic brain damage. *Brain Res Brain Res Rev,* **29,** 137-168.

Wang, L., Liu, Y. H., Huang, Y. G. and Chen, L. W. (2008). Time-course of neuronal death in the mouse pilocarpine model of chronic epilepsy using Fluoro-Jade C staining. *Brain Res,* **1241,** 157-167.

Wetherington, J., Serrano, G. and Dingledine, R. (2008). Astrocytes in the epileptic brain. *Neuron,* **58,** 168-178.

Yamada, M. and Hatanaka, H. (1994). Interleukin-6 protects cultured rat hippocampal neurons against glutamate-induced cell death. *Brain Res,* **643,** 173-180.

Yamada, T., Kawahara, K., Kosugi, T. and Tanaka, M. (2006). Nitric oxide produced during sublethal ischemia is crucial for the. *Neurochem Res,* **31,** 49-56.

Yoo, S. A., Bae, D. G., Ryoo, J. W., Kim, H. R., Park, G. S., Cho, C. S., Chae, C. B. and Kim, W. U. (2005). Arginine-rich anti-vascular endothelial growth factor (anti-VEGF) hexapeptide inhibits collagen-induced arthritis and VEGF-stimulated productions of TNF-alpha and IL-6 by human monocytes. *J Immunol,* **174,** 5846-5855.

Zhang, X., Gelowitz, D. L., Lai, C. T., Boulton, A. A. and Yu, P. H. (1997). Gradation of kainic acid-induced rat limbic seizures and expression of hippocampal heat shock protein-70. *Eur J Neurosci,* **9,** 760-769.